行政院國家科學委員會補助專題研究計畫 ■成果報告
□期中進度報告

穿心蓮調控解毒代謝酵素之研究

計畫類別：■個別型計畫　□整合型計畫
計畫編號：NSC 97-2320-B-039-047-MY3
執行期間： 97 年 08 月 01 日至 100 年 07 月 01 日

執行機構及系所：中國醫藥大學 營養學系

計畫主持人： 陳暉雯 教授

計畫參與人員：呂佳陽、楊瓊禎

成果報告類型(依經費核定清單規定繳交)：□精簡報告 ■完整報告

本計畫除繳交成果報告外，另須繳交以下出國心得報告：
□赴國外出差或研習心得報告
□赴大陸地區出差或研習心得報告
■出席國際學術會議心得報告
□國際合作研究計畫國外研究報告

處理方式：除列管計畫及下列情形者外，得立即公開查詢
□涉及專利或其他智慧財產權，□一年□二年後可公開查詢

中　華　民　國　100　年　07　月　22　日

目錄

中文摘要……..I

英文摘要……..II

報告內容……....III

第一部份: Activation of the cAMP/CREB/Inducible cAMP Early Repressor Pathway Suppresses Andrographolide-Induced Gene Expression of the π Class of Glutathione S-Transferase in Rat Primary Hepatocytes……...……1

第二部份: Andrographolide-induced pi class of glutathione S-transferase gene expression via PI3K/Akt pathway in rat primary hepatocytes……9

附件一、國科會補助專題研究計畫成果報告自評表……18

中文摘要

穿心蓮，又名苦心蓮，是在中國、韓國和印度等亞洲國家被廣泛使用的傳統中草藥，具有抗肝毒性、抗病毒、抗氧化與抗發炎等效果。穿心蓮內酯主要存在穿心蓮葉子中，是目前被發現穿心蓮中最具有生理活性的雙萜類之一。π 屬麩胱甘肽轉移酶(π class of glutathione *S*-transferase, GSTP)是生物轉換酵素系統中 phase II 酵素的一員，能代謝內生性和外生性親電性物質或自由基，以保護細胞免受外來毒物及致延誤的傷害。本實驗室先前研究證實，大鼠初代肝細胞處理穿心蓮乙醇萃出物、乙酸乙酯萃出物及穿心蓮內酯均可顯著誘發 GSTP mRNA 和蛋白質表現，且其調控 GSTP 表現機制可能與 PI3K/Akt 路徑相關；然而調控機制尚未完全釐清，因此本計畫以兩個部份來探討穿心蓮內酯對 GSTP 的調控機轉。第一部分的研究發現，穿心蓮內酯所誘發的 GSTP 表現會被 forskolin (cAMP 活化劑)和各種 cAMP 類似物所抑制，而這個抑制效應會在 PKA 的抑制劑 H89 處理下恢復，由此推論，cAMP/PKA 路徑在穿心蓮內酯誘發 GSTP 表現中可能扮演著負向調控的角色。此外，單獨處理 forskolin 或與穿心蓮內酯共同處理下會顯著增加胞內 ICER mRNA 表現。由以上的研究得知，當胞內 cAMP/PKA 路徑被刺激而大量活化時，ICER 在穿心蓮內酯誘發 GSTP 表現過程中扮演著負向調控的角色。第二部份研究是探討穿心蓮內酯是透過哪些分子機制影響 GSTP 的基因表現，結果指出，穿心蓮內酯會透過活化 PI3K/Akt 路徑活化 c-jun，進而增加細胞核中 activator protein-1 (AP-1)與 AP-1 核甘酸序列結合的親合力；且穿心蓮內酯所誘發的一系列反應都會受處理 PI3K 抑制劑 (LY294002 或 wortmannin)或將 PI3K 以 RNA 干擾的方式 knockdown 下而被抑制。綜合上述，在大鼠初代肝細胞中穿心蓮內酯是透過活化 PI3K/Akt 路徑活化 AP-1 與 GSTP 基因序列結合，進而促進 GSTP 表現；另外，cAMP/CREB/ICER 路徑在穿心蓮內酯誘發 GSTP 表現過程中扮演著負向調控的角色。

關鍵字: 穿心蓮內酯、cAMP/CREB/ICER pathway、PI3K/Akt pathway、π 屬麩胱甘肽轉移酶、初代肝細胞

Andrographis paniculata is an herb widely used in China, Korea, and India for its anti-hepatotoxic, anti-viral, and anti-inflammatory effects. Andrographolide is the major bioactive diterpene lactone in *A. paniculata*. The pi class of glutathione S-transferase (GSTP) is one of the phase II biotransformation enzymes. Our previous study indicated that andrographolide upregulates the expression of GSTP. Thus, this study is divided into two parts to clarify the mechanism by which andrographolide induces GSTP gene expression in rat primary hepatocytes. In part I, we indicated that induction of GSTP protein and mRNA expression in rat primary hepatocytes by andrographolide was inhibited by forskolin and a variety of cAMP analogues. Andrographolide alone had no effect on inducible cAMP early repressor (ICER) mRNA expression; however, andrographolide played a potentiating role in forskolin-induced ICER mRNA expression. An EMSA and immunoprecipitation assay showed that ICER binding to cAMP-response element (CRE) was increased in cells cotreated with andrographolide and forskolin. Taken together, these results suggest that ICER is likely to be involved in the suppression of andrographolide -induced GSTP expression caused by the increase of cAMP in rat primary hepatocytes. In part II, hepatocytes were treated with andrographolide, immunoblots showed maximal Akt phosphorylation at 0.5 h and maximal c-jun phosphorylation at 3 h. However, pretreatment with PI3K inhibitors, wortmannin and LY294002, or siPI3K inhibited the andrographolide-induced phosphorylation of c-jun and GSTP protein expression. EMSA showed that pretreatment with wortmannin, LY294002, or siPI3K attenuated the AP-1-DNA-binding activity caused by andrographolide. In summary, andrographolide induces GSTP gene expression in rat primary hepatocytes through activation of the PI3K/Akt, phosphorylation of c-jun, nuclear accumulation of AP-1, and subsequent binding to the response element in the gene promoter region.

Keywords: Andrographolide; cAMP/CREB/ICER pathway; PI3K/Akt pathway; π class of glutathione *S*-transferase (GSTP); primary hepatocytes

報告內容

- 發表刊物名稱、卷期及出版日期： **J. Agric. Food Chem. 2010, 58, 1993–2000**

JOURNAL OF AGRICULTURAL AND FOOD CHEMISTRY
ARTICLE

J. Agric. Food Chem. **2010,** *58,* 1993–2000 **1993**
DOI:10.1021/jf902221j

Activation of the cAMP/CREB/Inducible cAMP Early Repressor Pathway Suppresses Andrographolide-Induced Gene Expression of the π Class of Glutathione *S*-Transferase in Rat Primary Hepatocytes

Ai-Jen Yang,[†,∥] Chien-Chun Li,[‡,∥] Chia-Yang Lu,[†] Kai-Li Liu,[†] Chia-Wen Tsai,[§] Chong-Kuei Lii,*[,§] and Haw-Wen Chen*[,§]

[†]Department of Nutrition, Chung Shan Medical University, Taichung, Taiwan, [‡]Department of Nutrition and Health Sciences, Chang Jung Christian University, Tainan, Taiwan, and [§]Department of Nutrition, China Medical University, Taichung 404, Taiwan. [∥] These authors contributed equally to this work and therefore share first authorship.

Andrographolide (Ap) is a bioactive compound in *Andrographis paniculata* that is a Chinese herb. The π class of glutathione *S*-transferase (GSTP) is one kind of phase II detoxification enzyme. Here we show that induction of GSTP protein and mRNA expression in rat primary hepatocytes by Ap was inhibited by forskolin and a variety of cAMP analogues. The inhibitory effect of the cAMP analogues was partially blocked by pretreatment with H89. In the presence of Ap, forskolin, or both, the expression of phospho-cAMP response element-binding protein (CREB) was increased. Ap alone had no effect on inducible cAMP early repressor (ICER) mRNA expression; however, Ap played a potentiating role in forskolin-induced ICER mRNA expression. An EMSA and immunoprecipitation assay showed that ICER binding to cAMP-response element (CRE) was increased in cells cotreated with Ap and forskolin for 3 and 8 h. Taken together, these results suggest that ICER is likely to be involved in the suppression of Ap-induced GSTP expression caused by the increase of cAMP in rat primary hepatocytes.

KEYWORDS: Andrographolide; cAMP/CREB/ICER pathway; forskolin; π class of glutathione *S*-transferase (GSTP); hepatocytes

INTRODUCTION

The biotransformation enzyme system in mammals includes phase I and phase II enzymes and phase III membrane transporters that catalyze the conversion of xenobiotics to the polar metabolites that are more readily excreted (*1*). The glutathione *S*-transferases (GSTs) are phase II detoxification enzymes and are composed of two enzyme families with distinct catalytic and noncatalytic binding properties. One enzyme family consists of membrane-bound enzymes such as microsomal GST and leukotriene C4 synthetase; the other enzyme family consists of cytosolic enzymes that are encoded by at least five distantly related gene classes, namely, α, μ, π, σ, and θ (*2*). The π class of GST (GSTP) is one of the super families of GST enzymes that catalyze the conjugation of GSH to electrophilic xenobiotics, which results in the detoxification of electrophiles such as genotoxic chemical carcinogens and cytotoxic chemotherapeutic agents (*3*−*5*).

In most normal tissues, GSTP expression is very low; however, overexpression is frequently observed in several tumor tissues, including liver, brain, prostate, and lung (*4*,*6*), and in carcinomas such as lymphomas and synovial sarcoma (*7*). The overexpression of GSTP protein has been shown to be associated not only with anticancer drug resistance but also with increased tumor grade and tumor recurrence; moreover, high GSTP protein expression may lead to poor patient survival (*8*). GSTP is highly inducible during carcinogenesis, and the expression of GSTP is regarded as being an important determinant of cancer susceptibility and a reliable marker of tumorigenesis (*6*). Thus, the high levels of GSTP expression in tumors may be either a cause or an effect of the tumorigenic process.

The mechanisms underlying the regulation of GSTP expression during malignancy are highly complicated and not well understood. The GSTP gene has an enhancer element (GPE1; GSTP enhancer 1) at 2.5 kb upstream of the cap (*9*). In GPE1, there are two phorbol-12-*O*-tetradecanoate-13-acetate responsive element (TRE)-like elements that are considered to be required for the basal and inducible expression of GSTP (*10*). The transcriptional factor activator protein-1 (AP-1) has been shown to bind to the TREs and upregulate GSTP expression (*11*). The upregulation of GSTP expression by garlic allyl sulfides is dependent on both the c-Jun NH2-terminal kinase (JNK)-AP-1 and the extracellular receptor kinase (ERK)-AP-1 signaling pathways (*12*). In addition, a highly conserved sequence known as the cAMP response element (CRE), which is present in the 5′-region

*To whom correspondence should be addressed. H.-W.C.: tel, +886 4 22053366 ext. 7520; fax, +886 4 2206 2891; e-mail, chenhw@mail.cmu.edu.tw. C.-K.L.: tel, +886 4 22053366 ext. 7519; fax, +886 4 2206 2891; e-mail, cklii@mail.cmu.edu.tw.

Published on Web 01/11/2010 pubs.acs.org/JAFC

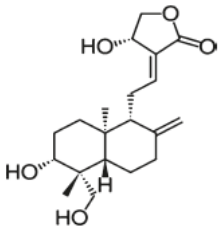

Figure 1. Chemical structure of andrographolide.

of the human GSTP gene, and cAMP- and cAMP response element-binding protein-1 (CREB-1)-mediated mechanisms are reported to be involved in the transcriptional regulation of the GSTP gene (*8*).

The CREB family belongs to the basic domain leucine zipper (bZIP) transcription factor class and comprises three members: CREB, CRE modulator (CREM), and activating transcription factor (ATF) (*13*). The CREB/CREM/ATF family members are homologous proteins that contain a basic DNA binding domain that recognizes the CRE (*14*). CREM encodes a variety of isoforms that are generated by alternative mRNA splicing. The isoforms function as either activators or repressors of cAMP-induced transcription (*15*). Inducible cAMP early repressor (ICER), an isoform of CREM, is a small protein of 120 amino acids and possesses only the bZIP domain (*16*). ICER plays a repressor role in cAMP-dependent transcription (*17*). Both CREB and ICER, members of the CREB family, are transcriptional regulators of the cAMP-mediated signaling pathway (*18*); however, they act in opposite ways. The ubiquitous transcription factor CREB binds to the CRE and activates target gene expression after the phosphorylation of its serine 133 by the cAMP-dependent PKA (*19*), and ICER competes with other bZIP proteins for the CRE and inhibits gene expression (*20*).

Andrographis paniculata (Bum. f) Nees, a Chinese herb, is a member of the Acanthaceae family. It is widely cultivated in Southeast Asia and is widely used as a traditional medicine in India, China, Thailand, and Scandinavia (*21*). *A. paniculata* was reported to have chemopreventive potential. In animal studies, administration of *A. paniculata* significantly increases hepatic activity of phase I (*22*) and phase II (*23*) enzymes. Andrographolide (Ap) (**Figure 1**) is the most abundant diterpene lactone in the leaves and stems of *A. paniculata* and has high biological activity and therapeutic potential (*24*). A clinical trial showed that Ap may inhibit HIV-induced cell cycle dysregulation and lead to a rise in $CD4^+$ lymphocyte levels in HIV-1 infected individuals (*25*). Many in vitro studies have indicated that Ap exerts anticancer activities, including antiangiogenesis (*26*), antiproliferation (*27*), and pro-apoptosis (*28*) effects. Our previous study showed that administration of ethanol or ethyl acetate extracts of *A. paniculata* and of Ap significantly increases GSTP expression in rat primary hepatocytes (*29*).

cAMP is a well-known intracellular second messenger, and it is known to play an important role in T-cell function (*30*). A variety of hormones, including glucagon, epinephrine, parathyroid, and adrenocorticotropic hormone (ACTH), were shown to increase intracellular cAMP level (*31*). In addition to its role in the immune system, cAMP has been shown to exert an inhibitory effect on the biotransformation enzyme system (*32*, *33*). In the present study, we used the rat primary hepatocyte culture system to study the role of increased cAMP as occurring in response to hormone stimulation in the modulation of Ap-induced GSTP expression which is an important component of the phase II enzyme system and the mechanisms underlying the regulation.

MATERIALS AND METHODS

Reagents and Antibodies. Cell culture medium (RPMI-1640) was purchased from Gibco-BRL (Gaithersburg, MD), collagenase type IV was obtained from Worthington Biochemical (Lakewood, NJ), Matrigel was purchased from Collaborative Biomedical Products (Bedford, MA), ITS™ Premix, collagen type I, and anti-GSTP antibody were purchased from BD Biosciences (San Jose, CA), anti-CREB (48H2), and antiphospho-CREB (ser133) antibodies were purchased from Cell Signaling Technology (Boston, MA), anti-CREM (ICER) was purchased from Santa Cruz Biotechnology, Inc. (Santa Cruz, CA), antimouse IgG (goat), antirabbit IgG (goat), and horseradish peroxidase-conjugated antibodies and enhanced chemiluminescence reagent were purchased from PerkinElmer Life Science, Inc. (Boston, MA), SP600125 (a JNK inhibitor) and PD98059 (an MAPK/ERK kinase inhibitor) were obtained from TOCRIS (Ellisville, MO), SB203580 (a p38 MAPK inhibitor) was purchased from Biosource (Camarillo, CA), antiactin monoclonal antibody, 8-bromo-cAMP, 8-(4-chlorophenylthio)-cAMP, dibutyryl-cAMP, forskolin, H89, 3-(4,5-dimethylthiazol-2-yl)-2,5-diphenyltetrazolium bromide (MTT), and all other chemicals were obtained from Sigma Chemical (St. Louis, MO). Taqman primer probes for GSTP, ICER, GAPDH, and Master Mixture were purchased from Applied Biosystems (Foster City, CA). Andrographolide was purchased from Calbiochem (Darmstadt, Germany).

Hepatocyte Isolation and Culture. Male Sprague−Dawley rats (weighing 250−300 g) were purchased from BioLASCO Taiwan Co., Ltd. (Taipei, Taiwan). Hepatocytes were isolated by a modification of the two-step collagenase perfusion method described previously (*34*). After isolation, hepatocytes (3×10^6 cells/dish) were plated on collagen-coated 60 mm plastic tissue dishes in RPMI-1640 medium (pH 7.38) supplemented with 10 mM HEPES, 1% ITS^+, 1 μM dexamethasone, 100 IU of penicillin/mL, and 100 μg of streptomycin/mL. Cells were incubated at 37 °C in a 5% CO_2 humidified incubator. After 4 h, cells were washed with PBS to remove any unattached or dead cells, the same medium was supplemented with Matrigel (233 mg/L), and 0.1 μM dexamethasone was added. Thereafter, the medium was changed daily. The protocol for each experiment is described in the corresponding figure legend. The rats were treated in compliance with the *Guide for the Care and Use of Laboratory Animals*.

Cell Viability. Cell viability was assessed by measuring the ability of viable cells to reduce a yellow MTT to a purple formazan by mitochondrial succinate dehydrogenase. After incubation with 40 μM andrographolide alone or in a combination of 40 μM andrographolide and various levels of forskolin for 48 h, the medium was removed, and hepatocytes were then incubated in RPMI-1640 medium containing 0.5 mg/mL MTT for an additional 3 h. The medium was then removed, and isopropyl alcohol was added to dissolve the formazan. After centrifugation at 9000*g* for 5 min, the supernatant of each sample was transferred to 96-well plates, and the absorbance was read at 570 nm in an ELISA reader. The absorbance in cultures treated with 0.1% DMSO (control) was regarded as 100% cell viability.

Intracellular cAMP Measurement. Intracellular cAMP concentrations were measured by using the cAMP EIA kit (Cayman Chemical). The cells were incubated with Ap or forskolin for 30 min, and cell extracts were prepared as described by Li et al. (*33*).

Nuclear Extracts Preparation. After each experiment, hepatocytes were washed twice with cold PBS and were then scraped from the dishes with 800 μL of PBS. Cell homogenates were centrifuged at 1800*g* for 5 min. The supernatant was discarded, and the cell pellet was allowed to swell on ice for 15 min after the addition of 200 μL of hypotonic extraction buffer containing 10 mM HEPES, 1 mM $MgCl_2$, 1 mM EDTA, 10 mM KCl, 0.5 mM dithiothreitol (DTT), 0.5% Nonidet P-40, 4 μg/mL leupeptin, 20 μg/mL aprotinin, and 0.2 mM phenylmethylsulfonyl fluoride (PMSF). After centrifugation at 7000*g* for 15 min, the resulting supernatant was discarded, and the pellet containing nuclei was extracted by gentle mixing with 50 μL of hypertonic extraction buffer containing 10 mM HEPES, 0.4 mM KCl, 1 mM $MgCl_2$, 1 mM EDTA, 0.5 mM DTT, 4 μg/mL leupeptin, 20 μg/mL aprotinin, 0.2 mM PMSF, and 10% glycerol at 4 °C for 30 min. The samples were then centrifuged at 20000*g* for 15 min. The supernatant containing the nuclear proteins was collected and stored at −80 °C until the electrophoretic mobility shift assay (EMSA).

EMSA. EMSA was carried out as described previously (*35*). Six micrograms of nuclear extract, poly (dI-dC), and biotinylated double-stranded CRE consensus oligonucleotides (5′-AGAGATTGCCT-GACGTCAGAGAGCTAG-3′) were mixed with the binding buffer (LightShift EMSA Kit; Pierce Chemical Co., Rockford, IL) to a final volume of 20 μL, and the mixture was incubated at 27 °C for 30 min. An unlabeled double-stranded CRE oligonucleotide and a double-stranded NF-κB oligonucleotide (5′-AGTTGAGGCGACTTTCCCAGGC-3′) were used to confirm competitive binding and specific binding, respectively. The nuclear protein-DNA complex was separated by 6% Tris/boric acid/EDTA-polyacrylamide gel electrophoresis and was then transferred to Hybond N^+ membranes. The membranes were cross-linked by UV light for 10 min and were then treated with 20 μL of streptavidin-horseradish peroxidase for 20 min, and the nuclear protein-DNA bands were developed with a SuperSignal West Pico kit (Pierce Chemical Co.).

Immunoprecipitation. Nuclear extracts were diluted to 1 μg/μL with IP buffer (40 mM Tris-HCl [pH 7.5], 1% NP-40, 150 mM NaCl, 5 mM EGTA, 1 mM DTT, 1 mM PMSF, 20 mM NaF, 1 μg/mL aprotinin, 1 μg/mL leupeptin, and 1 mM sodium vanadate). The diluted nuclear extracts (60 μg) were then incubated with 0.6 μg anti-ICER or anti-CREB antibody for 12 h at 4 °C, mixed with 4 μL protein A-Sepharose suspension (0.1 mg/mL), and incubated for an additional 1 h. Immunoprecipitates were collected by centrifugation at 16 000*g* for 2 min. The pellet was washed three times with 200 μL of IP buffer and was then subjected to Western blotting.

Western Blotting. After each experiment, hepatocytes were washed twice with cold PBS and were then scraped from the dishes with 500 μL of phosphate buffer containing 7.4 mM K_2HPO_4, 2.6 mM KH_2PO_4, and 15 M KCl (pH 7.4). Cell homogenates were centrifuged at 20 000*g* for 30 min. The resulting supernatant was used as a cellular protein for Western blot analysis. Nuclear extract proteins were prepared from rat primary hepatocytes as described above. For GSTP and actin, 4 μg of cellular proteins was used, for CREB and phospho-CREB, 30 μg of nuclear proteins was used, and for IP ICER and CREB, 60 μg of nuclear proteins was used. The protein samples were separated on 10% sodium dodecyl sulfate (SDS)−polyacrylamide gel, and the separated proteins were transferred to polyvinylidene diflouride membranes. After blocking, the membrane was incubated with anti-GSTP antibody (1:2000) and antiactin antibody (1:2000) for 45 min at room temperature, with anti-CREB antibody (1:2000) and antiphospho-CREB antibody (1:2000) for 1.5 h at room temperature, and with anti-ICER antibody (1:1000) for 12 h at 4 °C, followed by incubation with horseradish peroxidase-conjugated antibody for 1 h at room temperature. The protein bands were visualized by enhanced chemiluminescence plus Western blotting detection reagent (PerkinElmer Life Science, Inc.).

RNA Isolation and Real-Time PCR. Total RNA was isolated from rat primary hepatocytes by using TRIzol reagent (Invitrogen, Carlsbad, CA). Amounts of 0.8 μg of total RNA were reverse-transcribed with superscript II reverse transcriptase (Stratagene, Heidelberg, Germany) in a 20 μL final volume of reaction buffer, which consisted of 5 mM $MgCl_2$, 1 mM of each deoxyribonucleotide triphosphate, 2.5 U RNase inhibitor, and 2.5 mM oligo (dT). For the synthesis of cDNA, the reaction mixtures were incubated at 45 °C for 15 min; the reaction was stopped by denaturing the reverse transcriptase by heating the mixture to 99 °C for 5 min. For real-time PCR reactions, each sample was run in triplicate, and each 20 μL reaction contained 1 μL of GSTP (Rn02770492_gH), ICER (Rn00569145_m1), or GAPDH (Mm99999915_gl) Taqman primer probes and 10 μL of Taqman Master mixture, 5 μL of sample cDNA, and 4 μL of ddH_2O. Real-time PCR was performed on an SDS-7500 PCR instrument (Applied Biosystems). The real-time PCR runs consisted of first 1 cycle at 50 °C for 2 min, then 1 cycle at 95 °C for 10 min, and then 40 cycles at 95 °C for 15 s and 60 °C for 1 min. After cycling, relative quantification of mRNA against an internal control, GAPDH, was conducted according to the ΔC_T method (*36*).

Statistical Analysis. Data were analyzed by using analysis of variance (SAS Institute, Cary, NC). The significance of the difference between mean values was determined by one-way analysis of variance and Tukey's test; $p < 0.05$ was taken to be statistically significant.

RESULTS AND DISCUSSION

Cell Viability. The MTT assay was used to test whether the concentrations of Ap or Ap and forskolin used caused cell damage. There were no adverse effects on the growth of rat primary hepatocytes under these experimental conditions (**Figure 2**). In our study, the effects of Ap or Ap and forskolin observed were not due to cell viability.

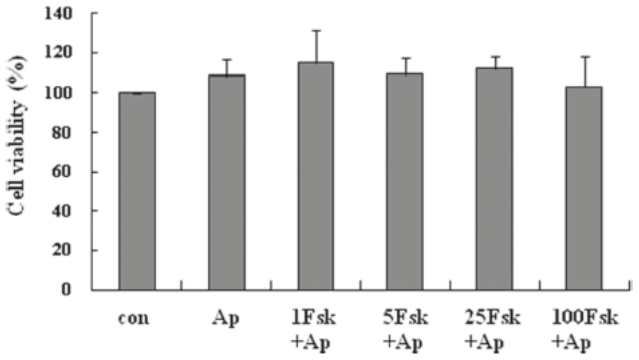

Figure 2. Effects of 40 μM Ap and of 40 μM Ap in combination with various concentrations of forskolin on cell viability. Results represent the mean ± SD ($n = 3$).

Ap-Induced GSTP Protein Expression Was Suppressed by Forskolin. To investigate the possible mechanisms involved in the induction of GSTP expression by Ap, we used MAPK inhibitors such as 25 μM PD98059 (an ERK1/2 inhibitor), 20 μM SP600125 (a JNK inhibitor), 20 μM SB203580 (a p38 MAPK inhibitor), and 25 μM forskolin (an adenylate cyclase activator). As shown in **Figure 3A**, 40 μM Ap significantly induced GSTP protein expression in rat primary hepatocytes and 25 μM forskolin significantly abolished this effect of Ap. The MAPK inhibitors, however, had no effect on GSTP protein expression induced by Ap (**Figure 3A**), which suggests that the ERK, JNK, and p38 MAPK pathways are not involved in the Ap-induced GSTP expression in rat primary hepatocytes. The concentrations of pharmacological inhibitors of ERK, JNK, and p38 MAPK we used were shown to be effective for their respective inhibitory functions in a previous study (*37*).

A dose−response inhibitory effect of forskolin (1−100 μM) on Ap-induced GSTP expression was further performed in rat primary hepatocytes. As shown in **Figure 3B,C**, forskolin suppressed Ap-induced GSTP expression in a dose-dependent manner, and a significant inhibition of both protein and mRNA levels was noted at doses ≥5 μM. These results imply that the downstream pathway of forskolin may be involved in the suppression of Ap-induced GSTP expression.

Ap-Induced GSTP Expression Was Suppressed by cAMP Analogues. Forskolin is known to increase intracellular cAMP and further activate cAMP-mediated signaling pathways (*38*). A previous study reported that treatment of hepatocytes with either forskolin or cAMP analogues results in a rapid and dramatic elevation of intracellular cAMP levels within 20 min (*39*). Increases of intracellular cAMP levels activates PKA and leads to suppression of the expression of phase I enzymes such as cytochrome P450 (CYP) 2B1 and CYP 3A1 in rat primary hepatocytes (*32*). Three highly membrane-permeable cAMP analogues, including dibutyryl-cAMP (DBT), 8-bromo-cAMP (Bromo), and 8-(4-chlorophenylthio)-cAMP (CPT), were tested to examine whether the effect of forskolin on GSTP expression was mediated by intracellular cAMP. As shown in **Figure 4A**, 1 and 10 μM DBT, 10 and 25 μM Bromo, and 0.5 and 2.5 μM CPT all significantly suppressed Ap-induced GSTP protein expression, and the inhibitory potency of the cAMP analogues was associated with their concentration. The GSTP mRNA expression pattern was similar to that of the protein (**Figure 4B**), although only the higher concentration of the cAMP analogues showed a significant effect.

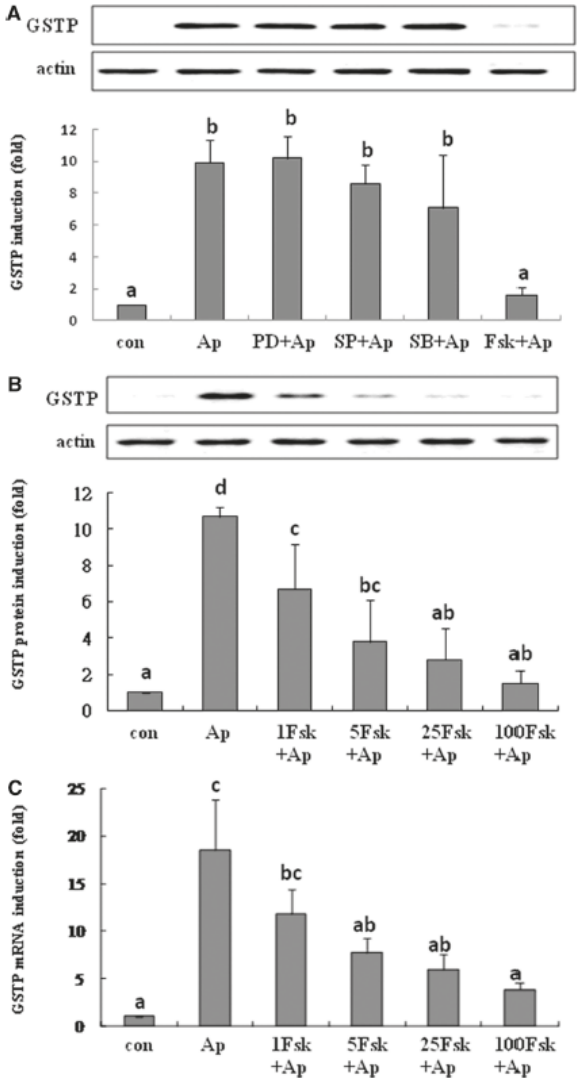

Figure 3. Effects of MAPK inhibitors and various concentrations of forskolin on Ap-induced GSTP expression. (**A**) Twenty-four hours after attachment, hepatocytes were pretreated with or without 25 μM PD98059 (PD), 20 μM SP600125 (SP), 20 μM SB203580 (SB), and 25 μM forskolin (Fsk) for 1 h before the addition of Ap. Cells were then treated with Ap for an additional 48 h. (**B**) Twenty-four hours after attachment, hepatocytes were pretreated with or without 1, 5, 25, or 100 μM forskolin (Fsk) for 1 h and were then incubated with 40 μM Ap for another 48 h. Aliquots of total protein (4 μg) were used for Western blot analysis. One representative experiment out of three independent experiments is shown (upper panel). Results represent the mean ± SD of three independent experiments (lower panel). Bars with different letters are significantly different ($p < 0.05$). (**C**) Aliquots of total RNA (0.8 μg) isolated from hepatocytes were subjected to real-time PCR analysis. Values of GSTP mRNA induction were normalized to the GAPDH mRNA level. Results represent the mean ± SD ($n = 3$). Bars with different letters are significantly different ($p < 0.05$).

The changes of intracellular cAMP concentration following Ap and forskolin treatments were monitored, and results showed that both Ap and forskolin significantly increased intracellular cAMP concentrations in comparison with the control group (**Figure 4C**). The intracellular cAMP concentration was 82-fold that of the control with forskolin treatment. An increase of cAMP concentration was also noted in Ap-treated cells, and the intracellular cAMP level was 22-fold that of the control.

PKA Inhibitor Reversed the Suppression of cAMP analogues on Ap-Induced GSTP Expression. The cAMP-dependent PKA pathway is involved in the regulation of the expression of genes such as

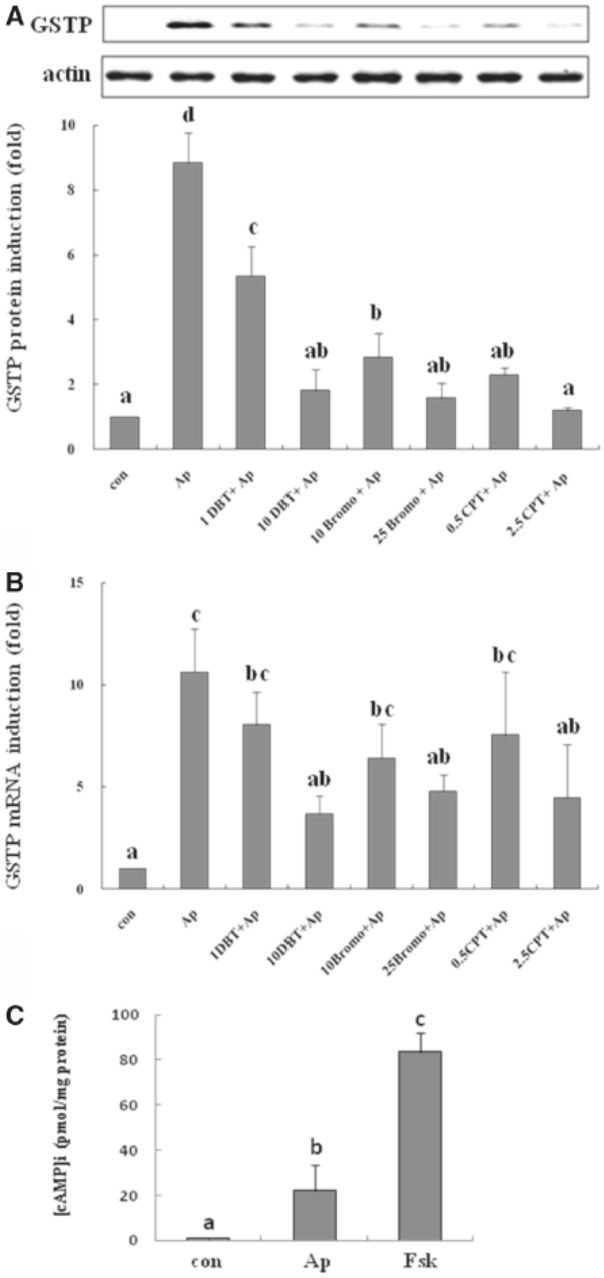

Figure 4. Effects of cell-permeable cAMP analogues on Ap-induced GSTP protein and mRNA expression and the changes of Ap and forskolin on the intracellular cAMP concentration. Twenty-four hours after attachment, hepatocytes were pretreated with or without 1 and 10 μM dibutyryl-cAMP (DBT), 10 and 25 μM 8-bromo-cAMP (Bromo), and 0.5 and 2.5 μM 8-(4-chlorophenylthio)-cAMP (CPT) for 1 h and were then incubated with 40 μM Ap for another 48 h. Cells were prepared for (**A**) GSTP protein and (**B**) GSTP mRNA determination. Values of GSTP mRNA induction were normalized to the GAPDH mRNA level. (**C**) Intracellular cAMP concentration of cells treated with 40 μM Ap or 25 μM forskolin. Results represent the mean ± SD ($n = 3$). Bars with different letters are significantly different ($p < 0.05$).

those encoding CYP 1A1 phase I enzyme (*40*), nuclear receptors, such as glucocorticoid receptor-interacting protein 1 (*41*), and phase III transport systems, such as organic anion transporting polypeptide 2 (*42*). In the present study, we used H89, a PKA inhibitor, to test whether the suppression of GSTP expression by forskolin is mediated through a cAMP-dependent PKA pathway. As shown in **Figure 5**, H89 significantly attenuated the suppression of GSTP expression by 10 μM DBT and 25 μM Bromo in the

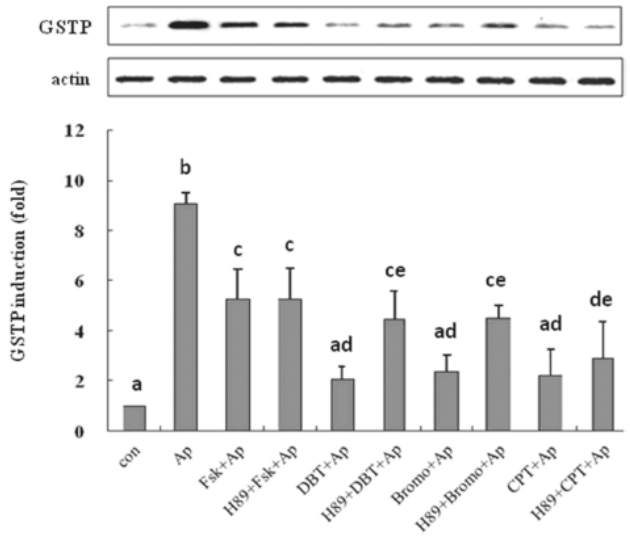

Figure 5. Effect of PKA inhibitor H89 on the suppression of GSTP protein expression by forskolin and cAMP analogues in the presence of Ap. Twenty-four hours after attachment, hepatocytes were pretreated with or without 7.5 μM H89 for 1 h and the cells were then treated with 5 μM forskolin (Fsk), 10 μM dibutyryl-cAMP (DBT), 25 μM 8-bromo-cAMP (Bromo), and 2.5 μM 8-(4-chlorophenylthio)-cAMP (CPT) for 1 h before the addition of Ap. Cells were then incubated with 40 μM Ap for another 48 h. One representative experiment out of three independent experiments is shown. Results in the lower panel represent the mean ± SD (n = 3). Bars with different letters are significantly different (p < 0.05).

presence of Ap, which suggests that the cAMP-dependent PKA pathway is involved in this suppression by cAMP. However, H89 only showed a partial effect in the 2.5 μM CPT group and did not reverse the inhibition of Ap-induced GSTP protein expression by 5 μM forskolin, which may be attributed to the ineffective concentration of H89 used.

Effects of Ap and Forskolin on the Phosphorylation of CREB. To investigate whether Ap and forskolin induced the phosphorylation of CREB in hepatocytes, we assayed the effect of 40 μM Ap, 25 μM forskolin, or both on CREB phosphorylation at 15 and 30 min. The results showed that the phosphorylation of CREB was significantly increased in rat primary hepatocytes treated with forskolin or Ap or both for 15 and 30 min (**Figure 6**). The phosphorylation of CREB by Ap and forskolin is quick response. This result is in line with that of a previous study, which showed that the phosphorylation of CREB by forskolin occurred rapidly and the peak in phosphorylation was achieved within 15 min, decay began in 30 min, and phosphorylation returned to the basal level after 8 h in H35 hepatoma cells (*43*).

Effects of Ap and Forskolin on ICER mRNA Level. ICER is a transcriptional repressor (*17*), and its competition with other bZIP proteins, such as CREB and ATF (*17*, *44*), accounts for its inhibitory effect on the expression of several genes, including CYP 19, CYP 51, Rab3a, Rab27 GTPase, Granuphilin/S1p4, and Noc2 (*45*−*47*). It was reported that the cAMP-mediated ICER expression depends on CREB phosphorylation (*48*). In this study, both Ap and forskolin were shown to significantly increase the intracellular cAMP levels (**Figure 4C**) and the phosphorylation of CREB (**Figure 6**). To investigate the role of ICER involved in the suppression of GSTP expression, we studied the effects of Ap and forskolin on ICER mRNA expression in rat primary hepatocytes. As indicated in **Figure 7**, ICER mRNA expression was increased by forskolin in a time-dependent manner. It was significantly increased after 2 h, and the increase was further

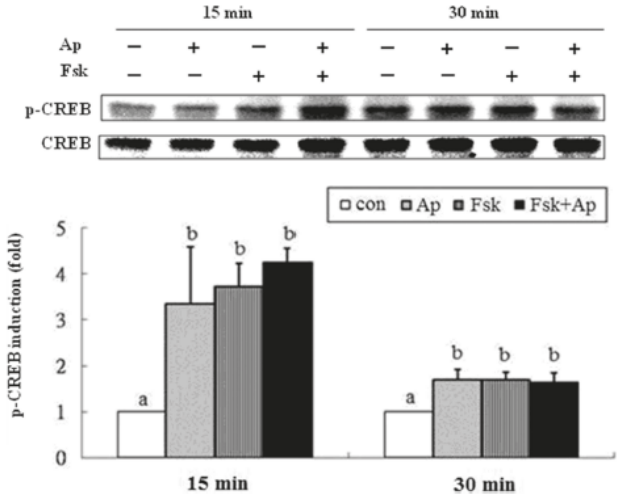

Figure 6. Effects of Ap and forskolin (Fsk) on CREB phosphorylation. Forty-eight hours after attachment, cells were treated with 40 μM Ap or 25 μM forskolin or cotreated with both Ap and forskolin for 15 or 30 min. After harvesting, aliquots of total protein (30 μg) were used for Western blot analysis. Results represent the mean ± SD (n = 3). Bars with different letters are significantly different within the group (p < 0.05).

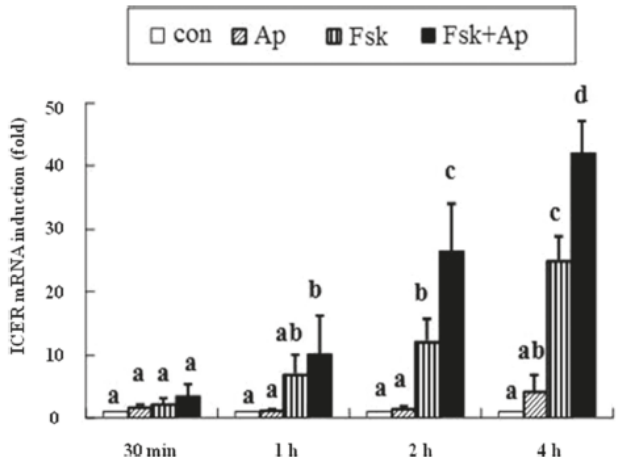

Figure 7. Effects of Ap and forskolin (Fsk) on the ICER mRNA level. Forty-eight hours after attachment, cells were treated with 40 μM Ap or 25 μM forskolin or cotreated with Ap and forskolin for 30 min or 1, 2, or 4 h. After harvesting, 0.8 μg of total RNA isolated from hepatocytes was subjected to real-time PCR analysis. Values of ICER mRNA induction were normalized to the GAPDH mRNA level. Results represent the mean ± SD (n = 3). Bars with different letters are significantly different (p < 0.05).

enhanced after 4 h (**Figure 7**). With Ap alone, ICER mRNA was not changed up to 4 h. However, in cells cotreated with forskolin and Ap, the expression of ICER mRNA was even greater than that of cells treated with forskolin alone. This finding suggests that there is a potentiating effect of Ap on forskolin-induced ICER mRNA expression and the inhibition of Ap-induced GSTP expression by forskolin in rat primary hepatocytes is likely related to the induction of ICER expression by forskolin.

ICER, a product of the CREM gene, is reported to be involved in an autoregulatory feedback loop of transcription that governs the suppression of early response genes, such as the proto-oncogene c-*fos* (*17*). Intriguingly, ICER mRNA expression was not induced by Ap; however, the induction of ICER mRNA expression was greater by Ap and forskolin cotreatment than by forskolin treatment alone (**Figure 7**). These results suggest that an

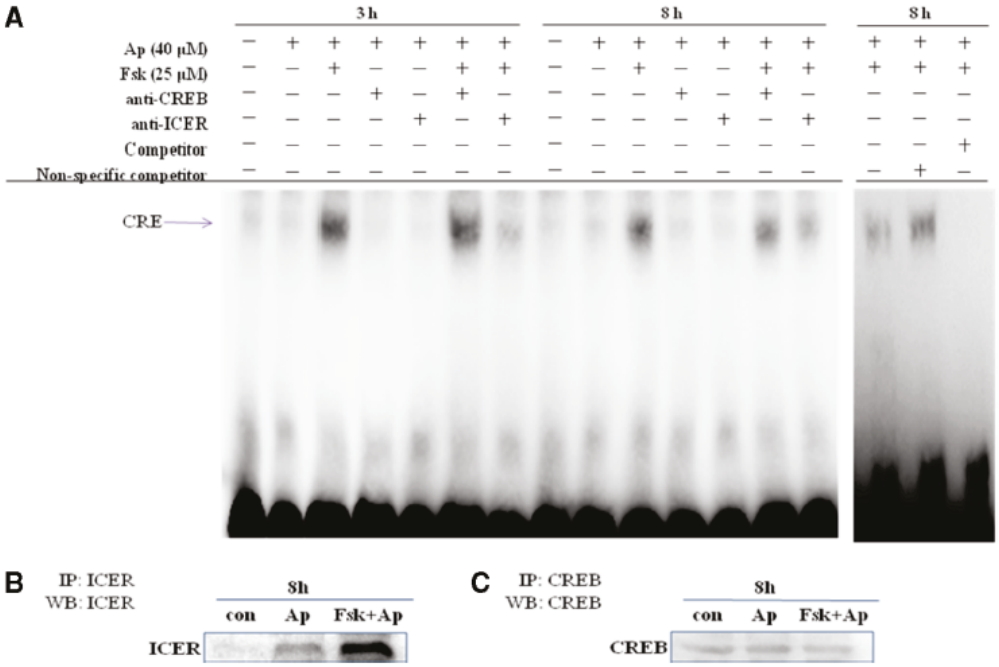

Figure 8. Identification of the component in the CRE complex by EMSA and immunoprecipitation (IP). Forty-eight hours after attachment, cells were treated with 40 μM Ap alone or cotreated with 40 μM Ap and 25 μM forskolin for 3 or 8 h. (**A**) Aliquots of total hepatocyte nuclear proteins (6 μg) were used for EMSA. To identify the protein bound to the CRE complex, either anti-CREB or anti-ICER antibody was added. To confirm the specificity of the nucleotides, 100-fold cold probe (biotin-unlabeled CRE) and NF-κB probe were included in the EMSA. One representative experiment out of three independent experiments is shown. The nuclear immunoprecipitates following antibody addition were subjected to Western blotting to confirm the presence of (**B**) ICER or (**C**) CREB in nuclear extracts.

interaction takes place between Ap and forskolin. Surprisingly, both Ap and forskolin significantly increased the intracellular cAMP level (**Figure 4C**), although forskolin showed a more potent effect and their effects on ICER formation were not consistent (**Figure 7**).

In a previous study (*49*), glucagon, glucagon-like peptide 1, and pituitary adenylyl cyclase-activating peptide all stimulate the formation of cAMP to a comparable extent in rat pancreatic islets, but only glucagon activates the expression of ICER. It was proposed that glucagon-like peptide 1 and pituitary adenylyl cyclase-activating peptide activate additional signal pathways that inhibit cAMP-mediated induction of ICER expression. For ICER formation, Ap may act in a manner similar to that for glucagon-like peptide 1 and pituitary adenylyl cyclase-activating peptide.

Effects of Ap and Forskolin on Nuclear CRE Complex Formation. In the present study, EMSA was performed to confirm whether the suppression of Ap-induced GSTP expression by forskolin was mediated by transcriptional factors binding to the CRE. As shown in **Figure 8A**, CRE complex formation was significantly increased in hepatocytes cotreated with Ap and forskolin for 3 and 8 h. To identify whether the component in the CRE complex was CREB or ICER, either anti-CREB or anti-ICER antibody was added to study their effects on EMSA. Results indicated that anti-ICER antibody apparently decreases nuclear protein binding to the CRE of cells cotreated with Ap and forskolin for 3 and 8 h (**Figure 8A**). In contrast, the binding of nuclear protein to the CRE was not affected by anti-CREB antibody. To further confirm the component in the CRE complex was ICER, the immunoprecipitates from nuclear extracts were thereafter subjected to SDS-PAGE and Western blotting. As shown, the amount of ICER in the nuclear immunoprecipitates was increased in cells cotreated with Ap and forskolin (**Figure 8B**); however, no effects of Ap and forskolin on CREB in the nuclear

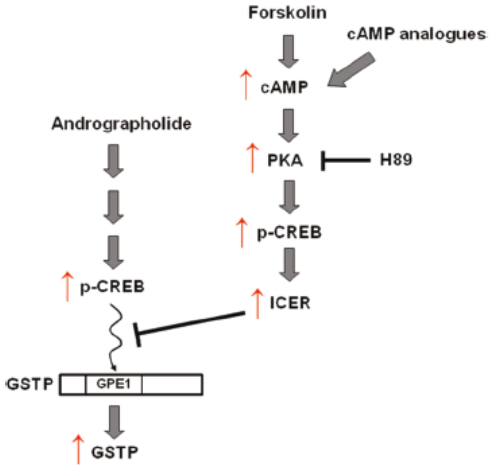

Figure 9. Model showing pathways that mediate cAMP suppresses Ap-induced GSTP expression in rat primary hepatocytes.

immunoprecipitates was found (**Figure 8C**). These results indicated that cotreatment with Ap and forskolin significantly increased nuclear ICER and subsequent binding to the CRE.

Although the intracellular cAMP level and the phosphorylation of CREB were increased by both Ap and forskolin (**Figure 4C**, **6**), the increased expression of ICER was only noted in cells treated with forskolin (**Figure 7**). Interestingly, the increase of ICER expression was even more significant in Ap- and forskolin-cotreated cells than in forskolin-treated cells. This raised the possibility that ICER or phospho-CREB/ICER protein ratio is likely to play a critical role in the suppression of Ap-induced GSTP expression by forskolin. The importance of phospho-CREB/ICER protein ratio in the transcriptional regulation of arylalkylamine *N*-acetyltransferase by norepinephrine has been reported in the rodent pineal gland (*50*).

The findings of the present study are schematically presented in **Figure 9**. This figure shows that Ap-induced expression of GSTP in rat primary hepatocytes is suppressed by an increase in cAMP level caused by forskolin, activation of cAMP/PKA pathway, phosphorylation of CREB, enhancement of ICER formation, binding of ICER to the CRE in the GSTP promoter, and concomitant attenuation of the CREB binding to the GPE1.

ABBREVIATIONS USED

Ap, andrographolide; AP-1, activator protein-1; ATF, activating transcription factor; ACTH, adrenocorticotropic hormone; bZIP, basic domain leucine zipper transcription factor; cAMP, 3,5′-cyclic adenosine monophosphate; CRE, cAMP-response element; CREB, cAMP response element-binding protein; CREM, CRE modulator; ERK, extracellular receptor kinase; ICER, inducible cAMP early repressor; JNK, c-Jun NH2-terminal kinase; GPE1, GSTP enhancer 1; GSTP, π class of glutathione *S*-transferase; MAPK, mitogen-activated protein kinase; PI3K, phosphatidylinositol 3-kinase; TRE, phorbol-12-*O*-tetradecanoate-13-acetate responsive element.

LITERATURE CITED

(1) Williams, R. T. Some recent studies on species variations in drug metabolism. *Chem. Biol. Interact*. **1971**, *3*, 311–312.

(2) Hayes, J. D.; Pulford, D. J. The glutathione S-transferase supergene family: regulation of GST and the contribution of the isoenzymes to cancer chemoprotection and drug resistance. *Crit. Rev. Biochem. Mol. Biol*. **1995**, *30*, 445–600.

(3) Townsend, D. M.; Tew, K. D. The role of glutathione-S-transferase in anti-cancer drug resistance. *Oncogene* **2003**, *22*, 7369–7375.

(4) Ritchie, K. J.; Henderson, C. J.; Wang, X. J.; Vassieva, O.; Carrie, D.; Farmer, P. B.; Gaskell, M.; Park, K.; Wolf, C. R. Glutathione transferase pi plays a critical role in the development of lung carcinogenesis following exposure to tobacco-related carcinogens and urethane. *Cancer Res*. **2007**, *67*, 9248–9257.

(5) Ikeda, H.; Nishi, S.; Sakai, M. Transcription factor Nrf2/MafK regulates rat placental glutathione S-transferase gene during hepatocarcinogenesis. *Biochem. J*. **2004**, *380*, 515–521.

(6) Dalhoff, K.; Buus Jensen, K.; Enghusen Poulsen, H Cancer and molecular biomarkers of phase 2. *Methods Enzymol*. **2005**, *400*, 618–627.

(7) Lopes, J. M.; Bruland, O. S.; Bjerkehagen, B.; Silva, M. C.; Holm, R.; Pettersen, E. O.; Solheim, O. P.; Sobrinho-Simões, M.; Nesland, J. M. Synovial sarcoma: immunohistochemical expression of P-glycoprotein and glutathione S transferase-pi and clinical drug resistance. *Pathol. Res. Pract*. **1997**, *193*, 21–36.

(8) Lo, H. W.; Ali-Osman, F. Cyclic AMP mediated GSTP1 gene activation in tumor cells involves the interaction of activated CREB-1 with the GSTP1 CRE: a novel mechanism of cellular GSTP1 gene regulation. *J. Cell. Biochem*. **2002**, *87*, 103–116.

(9) Okuda, A.; Imagawa, M.; Maeda, Y.; Sakai, M.; Muramatsu, M. Structural and functional analysis of an enhancer GPEI having a phorbol 12-O-tetradecanoate 13-acetate responsive elementlike sequence found in the rat glutathione transferase P gene. *J. Biol. Chem*. **1989**, *264*, 16919–16926.

(10) Matsumoto, M.; Imagawa, M.; Aoki, Y. Identification of an enhancer element of class Pi glutathione S-transferase gene required for expression by a co-planar polychlorinated biphenyl. *Biochem. J*. **1999**, *338*, 599–605.

(11) Angel, P.; Imagawa, M.; Chiu, R.; Stein, B.; Imbra, R. J.; Rahmsdorf, H. J.; Jonat, C.; Herrlich, P.; Karin, M. Phorbol ester-inducible genes contain a common cis element recognized by a TPA-modulated trans-acting factor. *Cell* **1987**, *49*, 729–739.

(12) Tsai, C. W.; Chen, H. W.; Yang, J. J.; Sheen, L. Y.; Lii, C. K. Diallyl disulfide and diallyl trisulfide up-regulate the expression of the pi class of glutathione S-transferase via an AP-1-dependent pathway. *J. Agric. Food Chem*. **2007**, *55*, 1019–1026.

(13) Hai, T. W.; Liu, F.; Coukos, W. J.; Green, M. R. Transcription factor ATF cDNA clones: An extensive family of leucine zipper proteins able to selectively form DNA-binding heterodimers. *Genes Dev*. **1989**, *3*, 2083–2090.

(14) Kim, M. K.; McClaskey, J. H.; Bodenner, D. L.; Weintraub, B. D. An AP-1-like factor and the pituitary-specific factor Pit-1 are both necessary to mediate hormonal induction of human thyrotropin beta gene expression. *J. Biol. Chem*. **1993**, *268*, 23366–23375.

(15) Laoide, B. M.; Foulkes, N. S.; Schlotter, F.; Sassone-Corsi, P. The functional versatility of CREM is determined by its modular structure. *EMBO J*. **1993**, *12*, 1179–1191.

(16) Servillo, G.; Della Fazia, M. A.; Sassone-Corsi, P. Coupling cAMP signaling to transcription in the liver: pivotal role of CREB and CREM. *Exp. Cell Res*. **2002**, *275*, 143–154.

(17) Misund, K.; Steigedal, T. S.; Laegreid, A.; Thommesen, L. Inducible cAMP early repressor splice variants ICER I and IIgamma both repress transcription of c-fos and chromogranin A. *J. Cell. Biochem*. **2007**, *101*, 1532–1544.

(18) Pigazzi, M.; Manara, E.; Baron, E.; Basso, G. ICER expression inhibits leukemia phenotype and controls tumor progression. *Leukemia* **2008**, *22*, 2217–2225.

(19) Brindle, P.; Nakajima, T.; Montminy, M. Multiple protein kinase A-regulated events are required for transcriptional induction by cAMP. *Proc. Natl. Acad. Sci. U.S.A*. **1995**, *92*, 10521–10525.

(20) Bernard, C.; Sutter, A.; Vinson, C.; Ratineau, C.; Chayvialle, J.; Cordier-Bussat, M. Peptones stimulate intestinal cholecystokinin gene transcription via cyclic adenosine monophosphate response element-binding factors. *Endocrinology* **2001**, *142*, 721–729.

(21) Bhan, M. K.; Dhar, A. K.; Khan, S.; Lattoo, S. K.; Gupta, K. K.; Choudhary, D. K. Screening and optimization of *Andrographis paniculata* (Burm.f.) Nees for total andrographolide content, yield and its components. *Sci. Hortic*. **2006**, *107*, 386–391.

(22) Jaruchotikamol, A.; Jarukamjorn, K.; Sirisangtrakul, W.; Sakuma, T.; Kawasaki, Y.; Nemoto, N. Strong synergistic induction of CYP1A1 expression by andrographolide plus typical CYP1A inducers in mouse hepatocytes. *Toxicol. Appl. Pharmacol*. **2007**, *224*, 156–162.

(23) Singh, R. P.; Banerjee, S.; Rao, A. R. Modulatory influence of Andrographis paniculata on mouse hepatic and extrahepatic carcinogen metabolizing enzymes and antioxidant status. *Phytother. Res*. **2001**, *15*, 382–390.

(24) Singha, P. K.; Roy, S.; Dey, S. Protective activity of andrographolide and arabinogalactan proteins from Andrographis paniculata Nees. against ethanol-induced toxicity in mice. *J. Ethnopharmacol*. **2007**, *111*, 13–21.

(25) Calabrese, C.; Berman, S. H.; Babish, J. G.; Ma, X.; Shinto, L.; Dorr, M.; Wells, K.; Wenner, C. A.; Standis, L. J. A phase I trial of andrographolide in HIV positive patients and normal volunteers. *Phytother. Res*. **2000**, *14*, 333–338.

(26) Sheeja, K.; Guruvayoorappan, C.; Kuttan, G. Antiangiogenic activity of Andrographis paniculata extract and andrographolide. *Int. Immunopharmacol*. **2007**, *7*, 211–221.

(27) Cheung, H. Y.; Cheung, S. H.; Li, J.; Cheung, C. S.; Lai, W. P.; Fong, W. F.; Leung, F. M. Andrographolide isolated from andrographis paniculata induces cell cycle arrest and mitochondrial-mediated apoptosis in human leukemic HL-60 cells. *Planta Med*. **2005**, *71*, 1106–1111.

(28) Zhao, F.; He, E. Q.; Wang, L.; Liu, K. Anti-tumor activities of a diterpene from Andrographis paniculata, by inducing apoptosis and inhibiting VEGF level. *J. Asian Nat. Prod. Res*. **2008**, *10*, 467–473.

(29) Chang, K. T.; Lii, C. K.; Tsai, C. W.; Yang, A. J.; Chen, H. W. Modulation of the expression of the pi class of glutathione S-transferase by Andrographis paniculata extracts and andrographolide. *Food Chem. Toxicol*. **2008**, *46*, 1079–1088.

(30) Barabitskaja, O.; Foulke, J. S., Jr.; Pati, S.; Bodor, J.; Reitz, M. S., Jr. Suppression of MIP-1beta transcription in human T cells is regulated by inducible cAMP early repressor (ICER). *J. Leukoc. Biol*. **2006**, *79*, 378–387.

(31) Cooper, B.; Gregerman, R. I. Hormone-sensitive fat cell adenylate cyclase in the rat. Influences of growth, cell size, and aging. *J. Clin. Invest*. **1976**, *57*, 161–168.

(32) Sidhu, J. S.; Omiecinski, C. J. cAMP-associated inhibition of phenobarbital-inducible cytochrome P450 gene expression in

primary rat hepatocyte cultures. *J. Biol. Chem.* **1995**, *270*, 12762–12773.
(33) Li, C. C.; Shen, H. L.; Lii, C. K.; Liu, K. L.; Yang, J. J.; Chen, H. W. Prostaglandin E2 down-regulation of cytochrome P-450 2B1 expression induced by phenobarbital is through EP2 receptor in rat hepatocytes. *Biochem. Biophys. Res. Commun.* **2005**, *327*, 424–430.
(34) Seglen, P. O. Preparation of isolated rat liver cells. *Methods Biol.* **1976**, *13*, 29–83.
(35) Li, C. C.; Lii, C. K.; Liu, K. L.; Yang, J. J.; Chen, H. W. DHA down-regulates phenobarbital-induced cytochrome P450 2B1 gene expression in rat primary hepatocytes by attenuating CAR translocation. *Toxicol. Appl. Pharmacol.* **2007**, *225*, 329–336.
(36) Giulietti, A.; Overbergh, L.; Valckx, D.; Decallonne, B.; Bouillon, R.; Mathieu, C. An overview of real-time quantitative PCR: applications to quantify cytokine gene expression. *Methods* **2001**, *25*, 386–401.
(37) Menor, C.; Fernández-Moreno, M. D.; Fueyo, J. A.; Escribano, O.; Olleros, T.; Arriaza, E.; Cara, C.; Lorusso, M.; Di Paola, M.; Román, I. D.; Guijarro, L. G. Azathioprine acts upon rat hepatocyte mitochondria and stress-activated protein kinases leading to necrosis: protective role of N-acetyl-L-cysteine. *J. Pharmacol. Exp. Ther.* **2004**, *311*, 668–676.
(38) Dahle, M. K.; Myhre, A. E.; Aasen, A. O.; Wang, J. E. Effects of forskolin on Kupffer cell production of interleukin-10 and tumor necrosis factor alpha differ from those of endogenous adenylyl cyclase activators: possible role for adenylyl cyclase 9. *Infect. Immun.* **2005**, *73*, 7290–7296.
(39) Björnsson, O. G.; Sparks, J. D.; Sparks, C. E.; Gibbons, G. F. Regulation of VLDL secretion in primary culture of rat hepatocytes: involvement of cAMP and cAMP-dependent protein kinases. *J. Lipid Res.* **1992**, *33*, 1017–1027.
(40) Sadar, M. D.; Blomstrand, F.; Andersson, T. B. Phenobarbital induction of cytochrome P4501A1 is regulated by cAMP-dependent protein kinase-mediated signaling pathways in rainbow trout hepatocytes. *Biochem. Biophys. Res. Commun.* **1996**, *225*, 455–461.
(41) Hoang, T.; Fenne, I. S.; Cook, C.; Børud, B.; Bakke, M.; Lien, E. A.; Mellgren, G. cAMP-dependent protein kinase regulates ubiquitin-proteasome-mediated degradation and subcellular localization of the nuclear receptor coactivator GRIP1. *J. Biol. Chem.* **2004**, *279*, 49120–49130.
(42) Chen, C.; Cheng, X.; Dieter, M. Z.; Tanaka, Y.; Klaassen, C. D. Activation of cAMP-dependent signaling pathway induces mouse organic anion transporting polypeptide 2 expression. *Mol. Pharmacol.* **2007**, *71*, 1159–1164.
(43) Servillo, G.; Penna, L.; Foulkes, N. S.; Magni, M. V.; Della Fazia, M. A.; Sassone-Corsi, P. Cyclic AMP signalling pathway and cellular proliferation: induction of CREM during liver regeneration. *Oncogene* **1997**, *14*, 1601–1606.
(44) Masquilier, D.; Sassone-Corsi, P. Transcriptional cross-talk: nuclear factors CREM and CREB bind to AP-1 sites and inhibit activation by Jun. *J. Biol. Chem.* **1992**, *267*, 22460–22466.
(45) Morales, V.; Gonzalez-Robayna, I.; Hernandez, I.; Quintana, J.; Santana, P.; Ruiz de Galarreta, C. M.; Fanjul, L. F. The inducible isoform of CREM (inducible cAMP early repressor, ICER) is a repressor of CYP19 rat ovarian promoter. *J. Endocrinol.* **2003**, *179*, 417–425.
(46) Fink, M.; Acimovic, J.; Rezen, T.; Tansek, N.; Rozman, D. Cholesterogenic lanosterol 14alpha-demethylase (CYP51) is an immediate early response gene. *Endocrinology* **2005**, *146*, 5321–5331.
(47) Abderrahmani, A.; Cheviet, S.; Ferdaoussi, M.; Coppola, T.; Waeber, G.; Regazzi, R. ICER induced by hyperglycemia represses the expression of genes essential for insulin exocytosis. *EMBO J.* **2006**, *25*, 977–986.
(48) Spessert, R.; Rapp, M.; Jastrow, H.; Karabul, N.; Blum, F.; Vollrath, L. A differential role of CREB phosphorylation in cAMP-inducible gene expression in the rat pineal. *Brain Res.* **2000**, *864*, 270–280.
(49) Hussain, M. A.; Daniel, P. B.; Habener, J. F. Glucagon stimulates expression of the inducible cAMP early repressor and suppresses insulin gene expression in pancreatic beta-cells. *Diabetes* **2000**, *49*, 1681–1690.
(50) von Gall, C.; Lewy, A.; Schomerus, C.; Vivien-Roels, B.; Pevét, P.; Korf, H. W.; Stehle, J. H. Transcription factor dynamics and neuroendocrine signalling in the mouse pineal gland: a comparative analysis of melatonin-deficient C57BL mice and melatonin-proficient C3H mice. *Eur. J. Neurosci.* **2000**, *12*, 964–972.

Received for review June 27, 2009. Revised manuscript received December 24, 2009. Accepted December 27, 2009. This work was supported by NSC-97-2320-B-039-047-MY3.

- 發表刊物名稱、卷期及出版日期: **Food and Chemical Toxicology 49 (2011) 281–289**

Food and Chemical Toxicology 49 (2011) 281–289

Contents lists available at ScienceDirect

Food and Chemical Toxicology

journal homepage: www.elsevier.com/locate/foodchemtox

Andrographolide-induced pi class of glutathione *S*-transferase gene expression via PI3K/Akt pathway in rat primary hepatocytes

Chia-Yang Lu [a], Chien-Chun Li [b], Chong-Kuei Lii [c], Hsien-Tsung Yao [c], Kai-Li Liu [a], Chia-Wen Tsai [c], Haw-Wen Chen [c,*]

[a] Department of Nutrition, Chung Shan Medical University, Taichung, Taiwan
[b] Department of Nutrition and Health Sciences, Chang Jung Christian University, Tainan, Taiwan
[c] Department of Nutrition, China Medical University, Taichung, Taiwan

ARTICLE INFO

Article history:
Received 5 May 2010
Accepted 31 October 2010

Keywords:
Andrographolide
Activator protein 1 (AP-1)
c-Jun
Pi class of glutathione *S*-transferase (GSTP)
Phosphatidylinositol 3-kinase (PI3K)/Akt
Rat primary hepatocytes

ABSTRACT

Andrographis paniculata is an herb widely used in China, Korea, and India for its anti-hepatotoxic, anti-viral, and anti-inflammatory effects. Andrographolide is the major bioactive diterpene lactone in *A. paniculata*. The pi class of glutathione *S*-transferase (GSTP) is one of the phase II biotransformation enzymes. Our previous study indicated that andrographolide upregulates the expression of GSTP. The aim of this study was to investigate the mechanism by which andrographolide induces GSTP gene expression in rat primary hepatocytes. In hepatocytes treated with 40 μM andrographolide, immunoblots showed maximal Akt phosphorylation at 0.5 h and maximal c-jun phosphorylation at 3 h. However, pretreatment with PI3K inhibitors, wortmannin and LY294002, or siPI3K inhibited the andrographolide-induced phosphorylation of c-jun and GSTP protein expression. EMSA showed that pretreatment with wortmannin, LY294002, or siPI3K attenuated the AP-1-DNA-binding activity caused by andrographolide. Results of immunoprecipitation indicated that nuclear c-fos/c-jun heterodimer increases with andrographolide treatment. Addition of antibodies against c-jun and c-fos decreased nuclear protein bound to the AP-1 consensus DNA sequence. In summary, andrographolide induces GSTP gene expression in rat primary hepatocytes through activation of the PI3K/Akt, phosphorylation of c-jun, nuclear accumulation of AP-1, and subsequent binding to the response element in the gene promoter region.

1. Introduction

Andrographis paniculata (Burm. f.) Nees (Acanthaceae) (*A. paniculata*) is an herbal medicine that is widely used in China, India, and other Asian countries. Clinically, *A. paniculata* is used to treat the common cold, urinary infection, diarrhea, and infectious hepatitis (World Health Organization, 2002). Andrographolide, a diterpene lactone, is the major bioactive component of *A. paniculata* and has antibacterial, anti-inflammatory, anti-oxidative, and anti-hepatotoxic properties in rodents and in cell models (Abu-Ghefreh et al., 2009; Kapil et al., 1993; Li et al., 2009; Shen et al., 2000; Visen et al., 1993).

Glutathione *S*-transferase (GST) is one of the phase II enzymes of the biotransformation system, which is composed of phase I enzymes, phase II metabolizing enzymes, and phase III transporters (van Iersel et al., 1999; Xu et al., 2005). Recent studies have shown that *A. paniculata* has effects on the biotransformation system. *A. paniculata* was demonstrated to increase the enzyme activities of cytochrome P450 (CYP450) 1A1, 2B, and GST in mouse liver (Jarukamjorn et al., 2006; Singh et al., 2001). Furthermore, crude extracts of *A. paniculata* and andrographolide were shown to induce gene expression of the pi class of GST (GSTP) in rat primary hepatocytes (Chang et al., 2008).

Akt, which is also known as protein kinase B, plays a crucial role in mammalian cellular signaling pathways involved in the regulation of cell survival, apoptosis, glucose uptake, and glycogen metabolism. Phosphoinositide 3-kinase (PI3K) phosphorylates and activates Akt (Rosseland et al., 2008; Stephens et al., 1998; Wierod et al., 2007), and the PI3K/Akt signaling pathway is affected by numerous phytochemicals (Chen and Kong, 2005; Manson et al.,

Abbreviations: AP-1, activator protein 1; CYP450, cytochrome P450; DMSO, dimethylsulfoxide; EMSA, electrophoretic mobility shift assay; ERK, extracellular signal-regulated kinase; GPE1, GSTP enhancer 1; GST, glutathione *S*-transferase; GSTP, pi class of GST; HEPES, N-[2-hydroxythyl]piperazine-N′-[2-ethanesulfonic acid]; JNK, c-Jun NH2-terminal kinase; TRE, 12-*O*-tetradecanoate-13-acetate-responsive element.

* Corresponding author. Address: Department of Nutrition, China Medical University, No. 91 Hsueh-Shih Road, Taichung, Taiwan. Tel.: +886 4 2205 3366x 7520; fax: +886 4 2206 2891.
E-mail address: chenhw@mail.cmu.edu.tw (H.-W. Chen).

0278-6915/$ - see front matter © 2010 Elsevier Ltd. All rights reserved.
doi:10.1016/j.fct.2010.10.030

2007; Martin et al., 2004; Neergheen et al., 2009). A recent study showed that the PI3K/Akt pathway is blocked by apigenin in human ovarian cancer cells (Fang et al., 2005). By contrast, andrographolide was found to suppress cell apoptosis through activation of the PI3K/Akt pathway in human umbilical vein endothelial cells (Chen et al., 2004).

Activator protein 1 (AP-1), a transcription factor, is a hetero or homodimer of the Jun and Fos families. AP-1 binds to the consensus DNA sequence including the 12-*O*-tetradecanoate-13-acetate-responsive element (TRE) and AP-1 binding motifs (Angel and Karin, 1991; Nadori et al., 1997). The 5′ upstream region of the GSTP gene promoter contains the enhancer element termed GSTP enhancer 1 (GPE1), which includes a TRE-like sequence. AP-1 was shown to bind to the GPE1 fragment in GSTP owning to the presence of the TRE-like sequence in GPE1 (Angel et al., 1987; Okuda et al., 1989; Sakai et al., 1988). The mitogen-activated protein kinases including c-jun N-terminal kinase (JNK), extracellular signal-regulated kinase (ERK), and p38 are considered to activate AP-1, followed by binding to the response element in DNA, which leads to target gene expression (De Bosscher et al., 2003; Reddy and Mossman, 2002). Furthermore, Hou et al. (2009) indicated that the PI3K/Akt pathway is essential for increasing AP-1 DNA-binding activity. Those authors showed that the increased AP-1 activation was involved in the enhanced bone morphogenetic protein-2 expression caused by ultrasound in murine primary osteoblastic cells.

Our previous study showed that GSTP gene expression is upregulated by andrographolide in rat primary hepatocytes and that the PI3K inhibitor wortmannin abolishes the induction of GSTP expression by andrographolide (Chang et al., 2008). In the present study, we further investigate the transcription factor that is involved in the upregulation of GSTP expression by andrographolide and the activation of the PI3K/Akt signaling pathway in rat primary hepatocytes.

2. Materials and methods

2.1. Chemicals

Cell culture medium (RPMI-1640) and penicillin–streptomycin solution were from GIBCO-BRL (Gaithersburg, MD); collagen and ITS$^+$ (insulin, transferrin, selenium, bovine serum albumin, and linoleic acid) were from Collaborative Biomedical Products (Bedford, MA); collagenase type I was from Worthington Biochemical (Lakewood, NJ); TRIzol reagent was from Invitrogen (Carlsbad, CA); dexamethasone, HEPES, sodium bicarbonate, calcium chloride, wortmannin, and LY294002 (PI3K kinase inhibitors) were from Sigma–Aldrich, Inc. (St. Louis, MO); andrographolide was from Calbiochem (Darmstadt, Germany); anti-phospho-Akt, anti-Akt, anti-ERK1/2, anti-phospho-ERK1/2, anti-p38, and anti-phospho-p38 antibodies were from Cell Signaling Technology (Danvers, MA); anti-JNK1, anti-phospho-JNK1/2, anti-phospho-c-jun, anti-c-jun, and anti-c-fos antibodies were from Santa Cruz Biotechnology (Santa Cruz, CA); and the transfection reagent Dharmafect 1 was from Dharmacon (Lafayette, CO).

2.2. Hepatocyte isolation and culture

Male Sprague–Dawley rats (weighing 250–300 g) were purchased from the BioLASCO Taiwan Co. Ltd. (Taipei, Taiwan). Hepatocytes were isolated by a modification of the two-step collagenase perfusion method described previously (Seglen, 1976). After isolation, hepatocytes (3×10^6 cells per dish) were plated on collagen-coated 60-mm plastic tissue dishes in RPMI-1640 medium (pH 7.38) supplemented with 10 mM HEPES, 1% ITS$^+$, 1 μM dexamethasone, 100 IU penicillin/mL, and 100 μg streptomycin/mL. Cells were incubated at 37 °C in a 5% CO_2 humidified incubator. After 4 h, cells were washed with PBS to remove any unattached or dead cells, and the same medium supplemented with 1% ITS$^+$ and 0.1 μM dexamethasone was added. Thereafter, the medium was changed daily. The protocol for each experiment is described in the corresponding figure legend. The rats were treated in compliance with the *Guide for the Care and Use of Laboratory Animals*.

2.3. Western blotting

Cells were washed twice with cold PBS and were harvested in 200 μL of 20 mM potassium phosphate buffer (pH 7.0). Cell homogenates were centrifuged at 9000*g* for 30 min at 4 °C. The protein content of the supernatant was measured by using the Coomassie Plus Protein Assay Reagent Kit (Pierce Chemical Company, Rockford, IL). Sodium dodecyl sulfate polyacrylamide gels made with 7.5% polyacrylamide were prepared as described by Laemmli (1970). For Akt, and c-jun 20 μg of cellular protein was used, and for GSTP, 4 μg of cellular protein was used. After electrophoresis, the separated proteins were transferred to polyvinylidene difluoride membranes. The nonspecific binding sites in the membranes were blocked with 5% nonfat dry milk in 15 mM Tris–150 mM NaCl buffer (pH 7.4) at room temperature for 2 h. After blocking, the membrane was incubated with anti-phospho Akt, anti-phospho-JNK1/2, anti-phospho-ERK1/2, and anti-phospho-p38 and anti-phospho c-jun or anti-Akt, anti-JNK1, anti-ERK1/2, anti-p38, anti-c-jun, and anti-c-fos antibodies at 4 °C overnight. Thereafter, the membrane was incubated with the secondary peroxidase-conjugated anti-rabbit or anti-mouse IgG at 37 °C for 1 h, and the immunoreactive bands were developed by use of the Western Lightning™ Plus-ECL kit (PerkinElmer, Waltham, MA).

2.4. Gene silencing experiments

Transfection experiments with small interfering RNA (siRNA) against p85α, a regulatory subunit of PI3K, were performed using a smart-pool of four specific siRNAs (Dharmacon catalog # J-080078-05, Thermo Fisher Scientific, Lafayette, CO) targeting rat PI3K (NM_013005). The four siRNAs against the rat p85α gene are (1) ACCUAUUGCGAGGGAAA, (2) CGAGAUGCAUCCACUAAAA, (3) GAUAAUGCAUAAUCACGAU, and (4) UAUGAGGAAUACACUCGUA. A targeting control-pool siRNA was also tested. Cells were transfected with Dharmafect 1 according to the manufacturer's instructions. Cells were plated at a density of 1.2×10^6 cells in 3.5 cm^2 dishes one day before transfection with 20 nM p85α or non-targeting control-pool siRNA for 24 h. Cells were then treated with 40 μM andrographolide in RPMI-1640 medium. Cell samples were collected for Western blotting analysis and EMSA.

2.5. Preparation of nuclear extract

Rat primary hepatocytes were pretreated with or without PI3K inhibitors, wortmannin or LY294002, for 1 h and were then treated with dimethylsulfoxide (DMSO) or andrographolide for 3 h and were washed twice with cold PBS followed by scraping from the dishes with PBS. Cell homogenates were centrifuged at 2000*g* for 5 min. The supernatant was discarded, and the cell pellet was allowed to swell on ice for 15 min after the addition of 200 μL of hypotonic buffer containing 10 mM HEPES, 10 mM KCl, 1 mM $MgCl_2$, 1 mM EDTA, 0.5 mM DTT, 4 μg/mL leupeptin, 20 μg/mL aprotinin, 0.5% Nonidet P-40, and 0.2 mM phenylmethylsulfonyl fluoride. After centrifugation at 6000*g* for 15 min, pellets containing crude nuclei were resuspended in 50 μL of hypertonic buffer containing 10 mM HEPES, 400 mM KCl, 1 mM $MgCl_2$, 1 mM EDTA, 0.5 mM DTT, 4 μg/mL leupeptin, 20 μg/mL aprotinin, 10% glycerol, and 0.2 mM phenylmethylsulfonyl fluoride at 4 °C for 30 min. The samples were then centrifuged at 20,000*g* for 15 min. The supernatant containing the nuclear proteins was collected and stored at −80 °C until the electrophoretic mobility shift assay (EMSA).

2.6. Immunoprecipitation

Nuclear extracts were diluted to 1 μg/μL with IP buffer (40 mM Tris–HCl [pH 7.5], 1% NP-40, 150 mM NaCl, 5 mM EGTA, 1 mM DTT, 1 mM PMSF, 20 mM NaF, 1 μg/mL aprotinin, 1 μg/mL leupeptin, and 1 mM sodium vanadate). The diluted nuclear extracts (60 μg) were incubated with 0.8 μg anti-c-jun or anti-c-fos antibody for 16 h at 4 °C, then mixed with 4 μL protein A-Sepharose suspension (0.1 mg/mL), and incubated at 4 °C for an additional 1 h. Immunoprecipitates and the supernatants were collected by centrifugation at 16,000*g* for 2 min. The pellet was washed with 200 μL of IP buffer three times and was then subjected to Western blotting.

2.7. Electrophoretic mobility shift assay

EMSA was performed according to our previous study (Cheng et al., 2004). The LightShift Chemiluminescent EMSA Kit (Pierce Chemical Company, Rockford, IL) and synthetic biotin-labeled double-stranded AP-1 consensus oligonucleotides (forward: 5′-GCCTCAGCTGGTAAATGGATAA-3′; reverse: 5′-AAAGGCCCCAGAGCCAGCC-3′) were used to measure AP-1 nuclear protein–DNA-binding activity (Tsai et al., 2007). Four micrograms of nuclear extract, poly (dI–dC), and biotin-labeled double stranded AP-1 oligonucleotide were mixed with the binding buffer (LightShift EMSA Kit; Pierce Chemical Co., Rockford, IL) to a final volume of 20 μL, and the mixture was incubated at room temperature for 30 min. Unlabeled double-stranded AP-1 oligonucleotide and a mutant double-stranded oligonucleotide were used to confirm the protein-binding specificity. The nuclear protein–DNA complex was separated by electrophoresis on a 6% TBE–polyacrylamide gel and was then transferred to a Hybond–N$^+$ nylon membrane. The membranes were cross-linked by UV light for 10 min and were then treated with 20 μL of streptavidin-horseradish peroxidase for 20 min, and the nuclear protein–DNA bands were developed with a SuperSignal West Pico kit (Pierce Chemical Co.).

2.8. Determination of purity of andrographolide

For determining the purity of andrographolide, andrographolide was dissolved in acetonitrile to obtain a final concentration of 30 and 100 μg/mL, respectively. Ten microliters of acetonitrile and andrographolide solutions were injected onto a Hitachi-L7400 Series LC System (Tokyo, Japan) equipped with an ultraviolet (UV) detector set to 254 nm. An Agilent Eclipse-C8 reversed-phase column (5 μm, 150 × 3.0 mm) was used. The mobile phase consisted of acetonitrile (Solvent A) and de-ionized water (Solvent B). The flow rate was 0.5 mL/min, and the total running time was 60 min. The gradient system was 90% B to 10% B (0~45 min), 10% B to 90% B (45~50 min), 90% B to 90% B (50~60 min). The column temperature was at ambient temperature (25 °C). The retention time of andrographolide was 19.8 min. The purity of andrographolide was calculated by dividing the peak area of andrographolide by the sum of peak area of all measurable peaks (without the solvent peak) × 100%.

2.9. Statistical analysis

Data were analyzed by using analysis of variance (SAS Institute, Cary, NC). The significance of the difference among mean values was determined by one-way analysis of variance followed by the Tukey's test. *P* values <0.05 were taken to be statistically significant.

3. Results

3.1. Effect of andrographolide on Akt phosphorylation in rat primary hepatocytes

In our previous study, we found that andrographolide-induced GSTP gene expression was significantly inhibited by wortmannin, a PI3K inhibitor, in rat primary hepatocytes (Chang et al., 2008). To clarify the importance of the PI3K/Akt signaling pathway in the induction of GSTP by andrographolide, we treated rat primary hepatocytes with 40 μM andrographolide for 0, 0.25, 0.5, 1 and 3 h. As shown in Fig. 1A, a significant and maximal phosphorylation of Akt was observed after 0.5 h ($P < 0.05$), and phosphorylation declined thereafter. Furthermore, Akt phosphorylation was induced by andrographolide in a dose-dependent manner (Fig. 1B). Previous studies showed that the JNK and ERK signaling pathways participate in the induction of GSTP expression mediated by diallyl disulfide and diallyl trisulfide in rat primary hepatocytes (Tsai et al., 2007, 2005). However, as shown in Fig. 1C, we observed no significant phosphorylation of JNK, ERK, or p38 in rat primary hepatocytes treated with 40 μM andrographolide for 0, 0.25, 0.5, 1, and 3 h.

3.2. Effect of andrographolide on c-jun phosphorylation

AP-1 regulates the expression of a wide variety of genes involved in various biological processes, including cell proliferation, differentiation, transformation, apoptosis, inflammation, and immune responses (Reddy and Mossman, 2002). Our previous study showed that the upregulation of GSTP expression by diallyl disulfide and diallyl trisulfide is via an AP-1-dependent pathway (Tsai et al., 2007). To determine the role of AP-1 in andrographolide-induced GSTP expression, we assayed the phosphorylation of c-jun in hepatocytes treated with 40 μM andrographolide for 0, 0.5, 1, 3, and 6 h. As shown in Fig. 2, phosphorylation of c-jun began at 0.5 h and maximal activation of c-jun was observed at 3 h and declined thereafter.

3.3. Effects of PI3K inhibitors on andrographolide-induced c-jun phosphorylation

To demonstrate the important role of the PI3K/Akt pathway in c-jun activation, hepatocytes were pretreated with PI3K inhibitors, wortmannin and LY294002, for 1 h, followed by incubation with 40 μM andrographolide for another 3 h. As shown in Fig. 3, both inhibitors significantly inhibited andrographolide-induced c-jun phosphorylation.

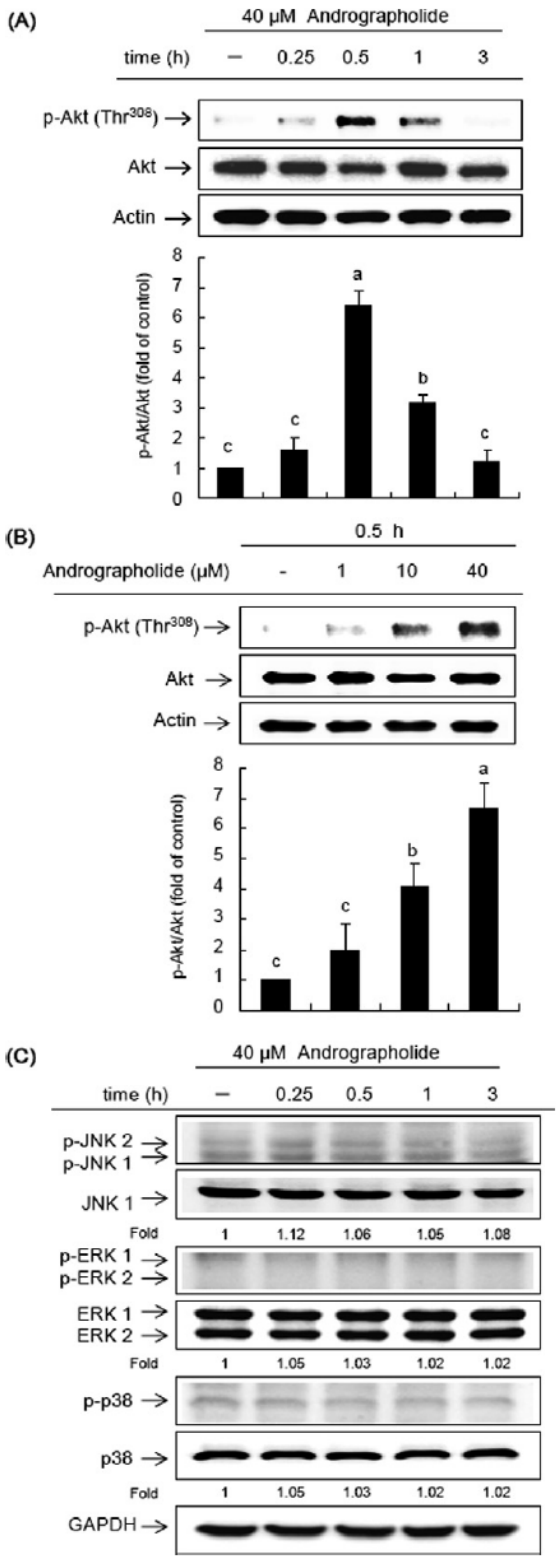

Fig. 1. Effect of andrographolide on Akt phosphorylation and MAPKs activation in rat primary hepatocytes. After attachment, (A) hepatocytes were treated with 40 μM andrographolide for various time periods and Akt phosphorylation was determined, (B) hepatocytes were exposed to various concentrations of andrographolide and Akt phosphorylation was determined, or (C) hepatocytes were treated with 40 μM andrographolide for various time periods and activation of various MAPKs was determined. Aliquots of total protein (20 μg) were used for Western blot analysis. Values are mean ± SD, $n = 3$. The levels in control cells were set at 1. Values not sharing the same letter are significantly different ($P < 0.05$).

3.4. Effect of PI3K siRNA on the andrographolide-induced phosphorylation of Akt and c-jun and GSTP expression

To further demonstrate the role of the PI3K signaling pathway in the regulation of andrographolide-induced GSTP gene expression, we transfected siRNA of p85α (siPI3K), a regulatory subunit of PI3K, in rat primary hepatocytes to knock down p85α. The efficiency of the siRNA SMARTpool system to knock down PI3K was assayed by Western blot (Fig. 4A). siPI3K abolished the andrographolide-induced phosphorylation of Akt and c-jun (Fig. 4B and C) and GSTP protein expression (Fig. 4D). These data suggest that PI3K/Akt-mediated c-jun activation is involved in the andrographolide-induced GSTP gene expression.

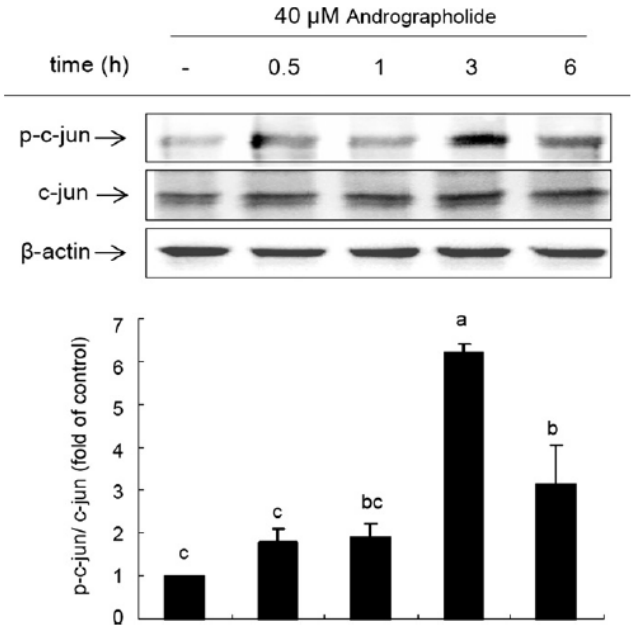

Fig. 2. Effect of andrographolide on c-jun phosphorylation in rat primary hepatocytes. After attachment, hepatocytes were treated with 40 μM andrographolide for various time periods. Aliquots of total protein (20 μg) were used for Western blot analysis. Values are mean ± SD, $n = 3$. The levels in control cells were set at 1. Values not sharing the same letter are significantly different ($P < 0.05$).

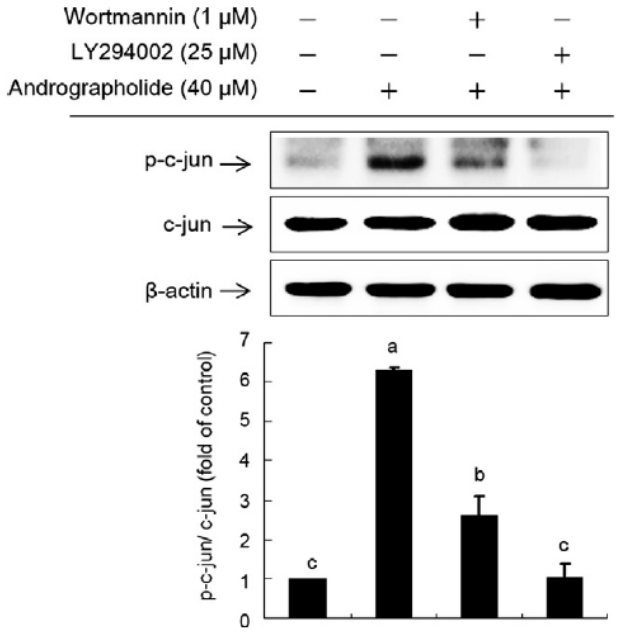

Fig. 3. Effects of PI3K inhibitors on andrographolide-induced c-jun phosphorylation in rat primary hepatocytes. After attachment, hepatocytes were pretreated with PI3K inhibitors, wortmannin and LY294002, for 1 h, and then treated with 40 μM andrographolide for another 3 h. Aliquots of total protein (20 μg) were used for Western blot analysis. Values are mean ± SD, $n = 3$. The levels in control cells were set at 1. Values not sharing the same letter are significantly different ($P < 0.05$).

3.5. Andrographolide induces AP-1 nuclear protein DNA-binding activity via the PI3K/Akt pathway in rat primary hepatocytes

As described above, activation of c-jun via the PI3K/Akt pathway is involved in andrographolide-induced GSTP expression in rat primary hepatocytes. We next performed an EMSA to determine whether the PI3K/Akt pathway plays an important role in andrographolide-mediated AP-1 DNA-binding activity. As shown in Fig. 5A, both PI3K inhibitors suppressed andrographolide-induced AP-1 nuclear protein DNA-binding complex formation. In

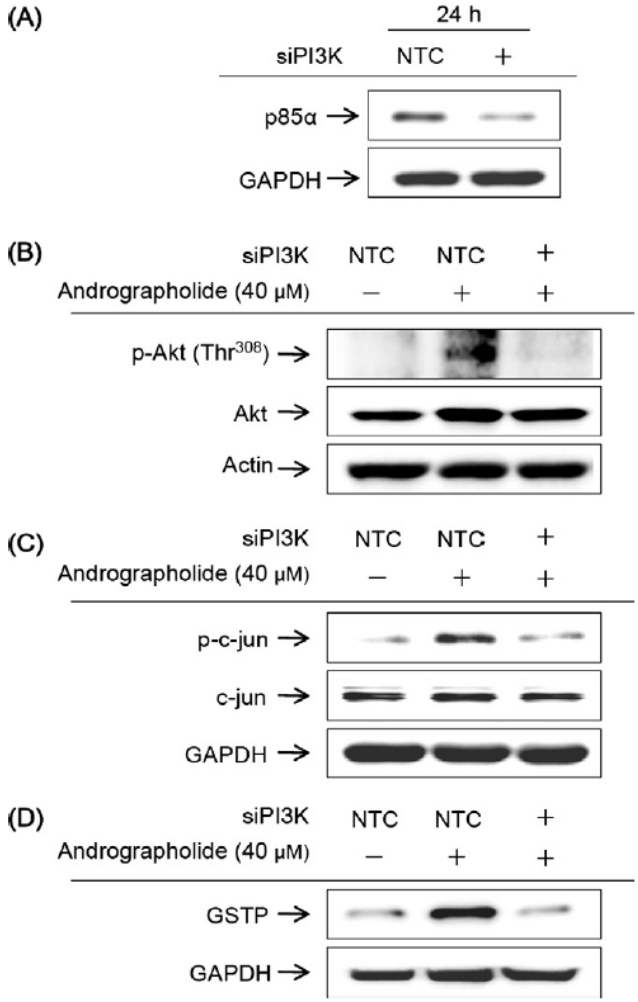

Fig. 4. Effect of PI3K siRNA on the andrographolide-induced phosphorylation of Akt and c-jun and GSTP expression in rat primary hepatocytes. After attachment, hepatocytes were transiently transfected with non-targeting control siRNA (NTC) or siPI3K for 24 h, followed by treatment with or without 40 μM andrographolide. Akt phosphorylation was observed at 0.5 h, c-jun phosphorylation was observed at 3 h, and GSTP expression was observed at 48 h. Aliquots of total protein (20 μg) were used for Western blot analysis. (A) Cells were transfected with non-targeting control siRNA or siPI3K for 24 h. (B) The blot was probed with anti-phospho-Akt (Thr^{308}) antibody. (C) The blot was probed with anti-phospho-c-jun antibody. (D) The blot was probed with anti-GSTP antibody. One representative immunoblot out of three independent experiments is shown.

addition, transient transfection with siPI3K abolished AP-1 nuclear protein DNA-binding complex formation (Fig. 5B).

3.6. c-Jun and c-fos involvement in andrographolide-induced AP-1 nuclear protein DNA-binding complex formation

As shown in Figs. 3A and 4C, the andrographolide-induced phosphorylation of c-jun was significantly inhibited by both PI3K inhibitors and siPI3K. Additionally, andrographolide-induced AP-1 nuclear protein DNA-binding complex formation was attenuated by both PI3K inhibitors and siPI3K (Fig. 5). AP-1 is a transcription factor mainly composed of Jun–Jun homodimer or Jun–Fos heterodimer (Reddy and Mossman, 2002). To further identify whether the nuclear proteins bound to the AP-1 binding site were c-jun and c-fos, we performed immunoprecipitation experiments with anti-c-jun or anti-c-fos antibody and a supershift experiment with anti-c-jun or anti-c-fos antibody, respectively. As shown in Fig. 6A, nuclear accumulation of c-fos after immunoprecipitation with anti-c-jun antibody and nuclear accumulation of c-jun after immunoprecipitation with anti-c-fos antibody were demonstrated in andrographolide-treated cells. This result suggested that nuclear

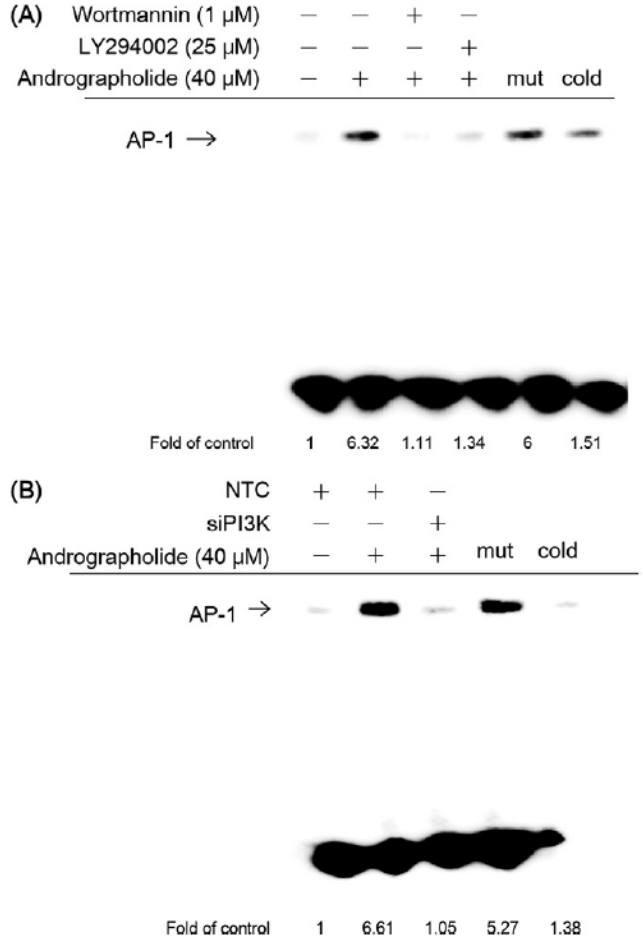

Fig. 5. Andrographolide induces AP-1 nuclear protein DNA-binding activity via the PI3K/Akt pathway in rat primary hepatocytes. After attachment, (A) hepatocytes were pretreated with PI3K inhibitors, wortmannin and LY294002, for 1 h or (B) were transiently transfected with non-targeting control siRNA or siPI3K for 24 h. After PI3K inhibitors or siRNA transfection, hepatocytes were treated with 40 μM andrographolide for an additional 3 h. Aliquots of nuclear extracts (4 μg) were used for EMSA. To confirm the specificity of the nucleotide, 600-fold cold probe (biotin-unlabeled AP-1 binding site) and biotin-labeled double-stranded mutant AP-1 oligonucleotide (2 ng) were included in the EMSA. One representative experiment out of three independent experiments is shown.

c-fos/c-jun heterodimer increases with andrographolide treatment. Although no supershift data observed, anti-c-jun and anti-c-fos antibodies decreased nuclear protein binding to the AP-1 oligonucleotide (Fig. 6B), and this implicated the components in nuclear protein binding to AP-1 oligonucleotide were c-jun and c-fos.

4. Discussion

GST, which is one of the phase II drug metabolizing enzymes, plays an important role in the biotransformation system. GST catalyzes the conjugation of glutathione with xenobiotic-derived and endogenous electrophiles and facilitates the excretion of conjugates. In mammalian cells, GST is classified into Alpha, Mu, Pi, Theta, Sigma, Kappa, and Omega classes (Lu, 1999; Sheehan et al., 2001; Zablotowicz et al., 1995). GSTP has been associated with the carcinogenic process and with anti-neoplastic drug resistance in cancer cells (Hayes and Pulford, 1995; Henderson et al., 1998). GSTP was recognized as a marker in several rat hepatocarcinogenesis models because of its over-expression within hepatocellular foci and neoplasms (Perez-Carreon, 2009). Several studies have addressed the regulation of GSTP expression, and previous studies have shown that hepatic GSTP is induced by both nutrient and non-nutrient factors (Chang et al., 2008; Chen et al., 2001; Liu et al., 2009; Milbury et al., 2007; Tsai et al., 2005).

Fourteen flavonoids and 13 diterpenoids have been isolated from *A. paniculata* (Chen et al., 2006a,b), and andrographolide is the most abundant diterpenoid. To determine the storage stability of andrographolide, the purity of andrograrpholide used was determined by HPLC. The results showed the purity of andrographolide crystalline is 98% (Fig. 7). Andrographolide has been shown to have anti-HIV, immunostimulatory, anti-inflammatory, and anti-hepatotoxic activities (World Health Organization, 2002). Li et al. (2007) indicated that andrographolide can induce cell cycle arrest at the G2/M phase and cell death in HepG2 cells. A recent study showed that andrographolide can inhibit the migration and invasion of human non-small-cell lung cancer cells (Lee et al., 2010). Such evidence suggests that andrographolide has anti-tumor cell growth properties and inhibits tumor progression. Andrographolide was also shown to have antioxidant activity via the upregulation of a large number of antioxidant enzymes, such as the γ-glutamate cysteine ligase catalytic subunit and modifier subunit (Woo et al., 2008). The effective dose of andrographolide in different biological processes varies depending on cell type. In the present study, we used 40 μM andrographolide to treat rat primary hepatocytes, which was a dose we found in our previous study not to inhibit cell growth (Yang et al., 2010). The tested compound andrographolide dissolves well in culture medium. We do not know whether 40 μM andrographolide is the physiologically achievable level, however, 1–40 μM andrographolide shows a dose-response effect on Akt phosphorylation (Fig. 1B). In our previous study, andrographolide (2.5–7.5 μM) was found to inhibit the TNF-α-induced expression of ICAM-1 in a dose-dependent manner and result in a decrease in HL-60 cell adhesion to EA.hy926 cells (Yu et al., 2010). We will try the lower concentration of andrographolide for a longer time period in our future study to determine the function of physiologically achievable level of andrographolide.

Andrographolide regulates the expression of different genes through distinct signal transduction pathways. In human cancer cells, andrographolide inhibits the Janus-activated kinase/signal transducers and activator of transcription 3 (JAK-STAT3) pathway and reduces its downstream protein expression, including Bcl-xL, Mcl-1, and cyclin D1 (Zhou et al., 2010). Lipopolysaccharide-induced TNF-α production is suppressed by andrographolide, and this effect is via its inhibition of the ERK1/2 pathway in mouse

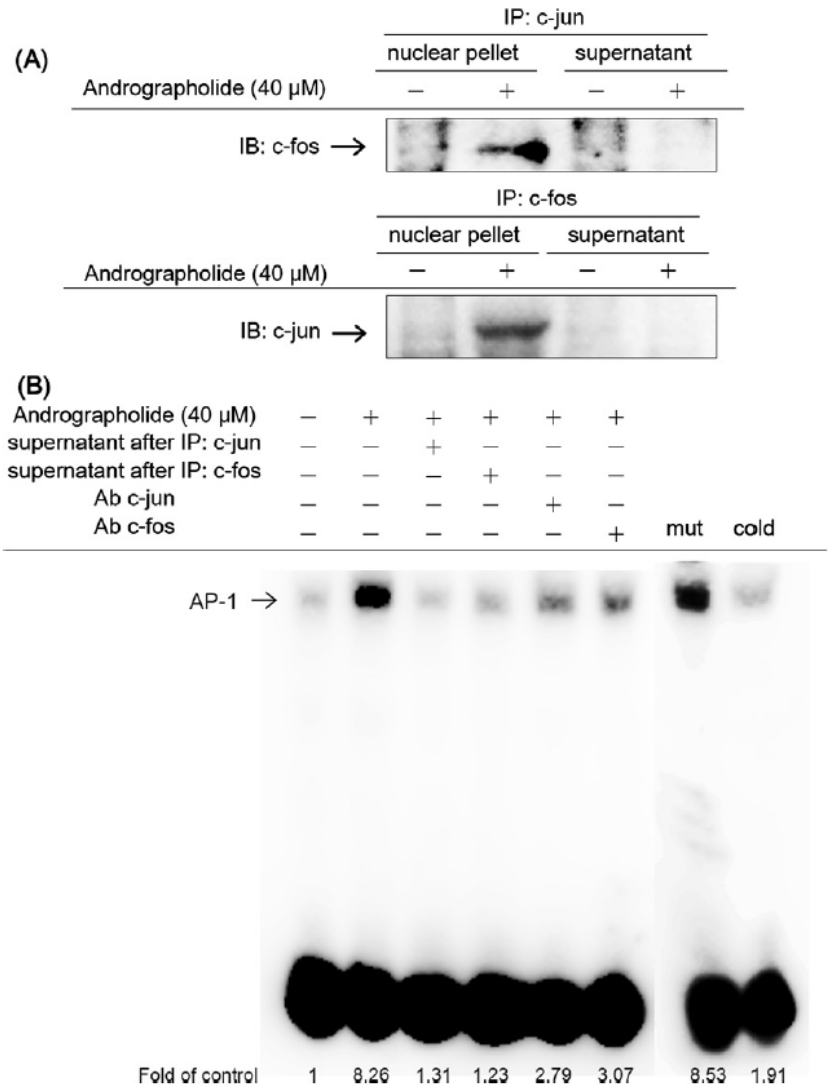

Fig. 6. Andrographolide-induced abundant constitutive c-jun and c-fos/AP-1 DNA-binding activity in rat primary hepatocytes. After attachment, hepatocytes were treated with or without 40 μM andrographolide for 3 h. (A) Immunoprecipitation of c-jun and c-fos in the nuclear extracts of andrographolide-treated cells. Western blot analysis was used to detect c-fos and c-jun protein in the pellets and supernatants which were pulled down by anti-c-jun and anti-c-fos antibodies, respectively. (B) Aliquots of nuclear extracts (8 μg) and the supernatants after immunoprecipitation with anti-c-jun or anti-c-fos antibodies were used for EMSA. To identify the proteins bound to the AP-1 binding site, anti-c-jun and anti-c-fos antibodies were used and EMSA supershift assay was performed. To confirm the specificity of the nucleotide, 600-fold cold probe (biotin-unlabeled AP-1 binding site) and biotin-labeled double-stranded mutant AP-1 oligonucleotide (2 ng) were included in the EMSA. One representative experiment out of three independent experiments is shown.

peritoneal macrophages (Qin et al., 2006). In addition, andrographolide inhibits the TNF-α-induced NF-κB signaling pathway and reduces the expression of the cell adhesion molecule E-selectin in human umbilical vein endothelial cells (Xia et al., 2004).

PI3K was found to activate phosphoinositide-dependent protein kinase-1 (PDK-1) and PDK-2 upon phosphorylation. Akt is a cytosolic protein that is recruited to the plasma membrane upon activation of PI3K (Andjelkovic et al., 1997). On the plasma membrane, Akt is phosphorylated by PDKs and then translocates through the cytosol to the nucleus (Andjelkovic et al., 1997). Akt has two phosphorylation residues, Thr^{308} and Ser^{473}. PDK-1 is identified to phosphorylate Thr^{308} of Akt, and PDK-2 phosphorylates Ser^{473} (Alessi et al., 1997). Many phytochemicals, such as curcumin, resveratrol, epigallocatechin-3-gallate, indole-3-carbinol, diindolylmethane, carnosol, and andrographolide, are considered to modulate the PI3K/Akt signaling pathway (Chang et al., 2008; Chen and Kong, 2005; Choi et al., 2008; Manson et al., 2007; Martin et al., 2004; Neergheen et al., 2009; Roy et al., 2009). For instance, curcumin was found to down-regulate P-glycoprotein expression by inhibiting the PI3K/Akt pathway in multidrug-resistant L1210/Adr cells (Choi et al., 2008). In another study, Roy et al. (2009) showed that resveratrol suppresses 7,12-dimethylbenz(*a*)anthracene-induced mouse skin tumorigenesis by abolishing the PI3K/Akt pathway. In addition, carnosol was found to upregulate HO-1 gene expression by activating the PI3K/Akt pathway (Martin et al., 2004). In our previous study, we showed that *A. paniculata* and its bioactive diterpene andrographolide upregulate GSTP gene expression in rat primary hepatocytes via the PI3K/Akt signaling pathway (Chang et al., 2008). Although the same result was found in the present study, we presented a new finding that PI3K/Akt activates AP-1 which is involved in andrographolide-induced GSTP expression (Fig. 5). In the present study, we found that andrographolide significantly induced phosphorylation of Thr^{308} of Akt (Fig. 1) and that wortmannin suppressed the andrographolide-induced GSTP expression, as reported previously (Chang et al., 2008). These findings suggest that the PI3K/PDK-1/Akt signaling pathway plays a

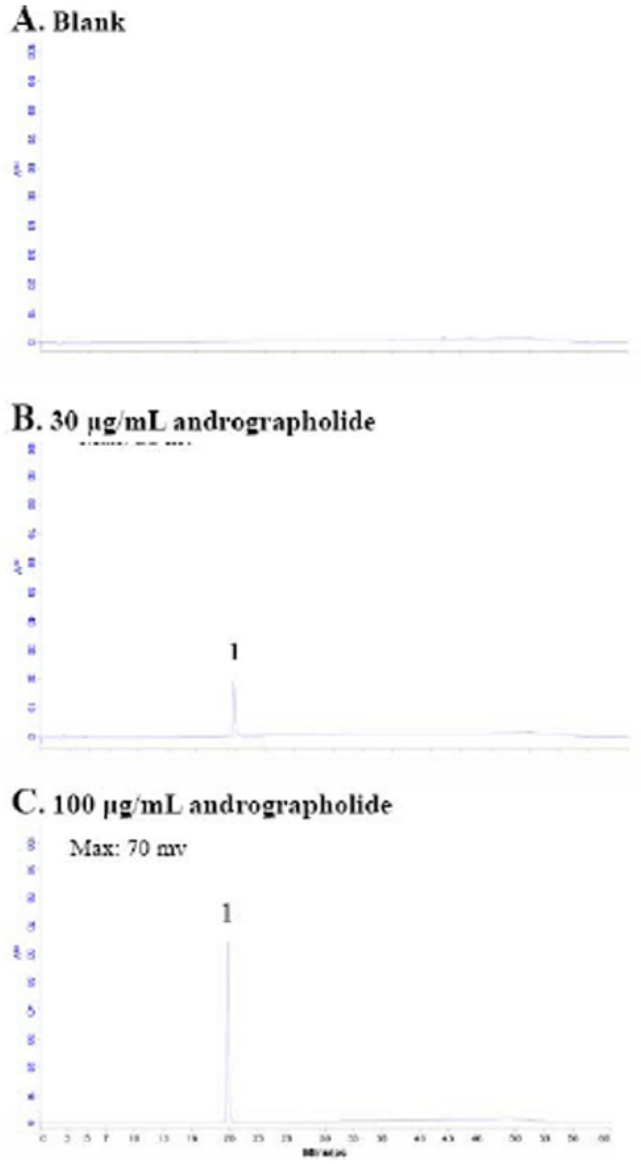

Fig. 7. HPLC/UV chromatograms of (A) blank (acetonitrile), (B) 30 μg/mL andrographolide, and (C) 100 μg/mL andrographolide. The retention time of peak 1 (andrographolide) was 19.8 min.

critical role in andrographolide-induced GSTP expression in rat primary hepatocytes.

AP-1 is one kind of transcription factor that modulates the expression of numerous genes involved in cellular adaptation, differentiation, and proliferation (Surh, 2003). Neergheen et al. (2009) indicated that resveratrol, gingerol, capsaicin, and ginsenosides can influence AP-1 activation. In human leukemia cells, c-jun was shown to bind to the GSTP gene promoter (Borde-Chiche et al., 2001). Tsai et al. (2007) suggested that AP-1 is an important transcription factor for GSTP gene expression by diallyl disulfide and diallyl trisulfide. In addition, sulforaphane, alpha-lipoic acid, and dihydrolipoic acid were shown to induce enzyme activity and gene expression of GSTP, and this induction was associated with the AP-1 and Nrf2 transcription factors (Lii et al., 2010).

Several studies have shown that GSTP gene expression is modulated by various phytochemicals through different signaling pathways, such as JNK, ERK, and p38 (Bergelson et al., 1994; Duvoix et al., 2004; Reddy and Mossman, 2002; Tsai et al., 2007). However, those pathways were not involved in the andrographolide-induced GSTP expression in our cell model system. Although the role of the PI3K/Akt signaling pathway in andrographolide-induced GSTP expression has been explored in rat primary hepatocytes (Chang et al., 2008), the downstream molecule of the PI3K/Akt pathway in this induction had not been identified. The results of Figs. 1 and 2 show that andrographolide can induce Akt and c-jun phosphorylation. These results suggest that AP-1 activation by andrographolide is possibly through the PI3K/Akt pathway rather than the MAPK pathway.

To further demonstrate the critical role of PI3K in andrographolide-induced GSTP gene expression, we used siPI3K to knock down the expression of PI3K and reduce its downstream molecule activation and the expression of its target genes. As shown in Figs. 4 and 5, siPI3K acted like the PI3K inhibitors wortmannin and LY294002 and suppressed the andrographolide-induced phosphorylation of Akt and c-jun, AP-1 DNA-binding activity, and GSTP expression. These data implicate the PI3K/Akt signaling pathway and the AP-1 transcription factor in andrographolide-induced GSTP gene expression.

We were also interested in investigating which transcription factor is the main target of the PI3K/Akt signaling pathway in the andrographolide induction of GSTP. Among the possible candidates, AP-1 seemed to be the most attractive because several lines of evidence have suggested the possible participation of AP-1/Jun family members in the regulation of GSTP gene expression by binding to the enhancer element GPE1 (Angel et al., 1987; Okuda et al., 1989; Sakai et al., 1988). In the present study, we noted a dramatic increase in c-jun phosphorylation (Fig. 2) and AP-1 translocation into the nucleus (Fig. 6A) as well as in the DNA-binding activity of AP-1 (Fig. 6B) in cells treated with andrographolide. c-Fos and c-jun are components of transcription factor AP-1, and fos/jun heterodimers are the most active. To identify whether the nuclear proteins bound to the AP-1 response element were c-jun and c-fos, we performed immunoprecipitation with anti-c-jun or anti-c-fos antibody and a supershift experiment with anti-c-jun or anti-c-fos antibody, respectively. As shown in Fig. 6A, nuclear accumulation of c-fos after immunoprecipitation with anti-c-jun antibody and nuclear accumulation of c-jun after immunoprecipitation with anti-c-fos antibody were demonstrated in andrographolide-treated cells. This result suggested that nuclear c-fos/c-jun heterodimer increases with andrographolide treatment. Anti-c-jun and anti-c-fos antibodies were used to perform the supershift experiment. Although no supershift data observed, anti-c-jun and anti-c-fos antibodies decreased nuclear protein binding to the AP-1 oligonucleotide (Fig. 6B). It might be because the anti-c-jun and anti-c-fos antibodies compete with AP-1 oligonucleotide for the same binding site on c-jun and c-fos. The results implicate the importance of c-jun and c-fos in andrographolide-induced AP-1 nuclear protein DNA-binding complex formation. Thus, we showed that AP-1 likely participates in upregulating GSTP transcription.

MAPKs are known to be the upstream activator of AP-1, and several studies have reported that GSTP gene expression is modulated by various phytochemicals through the MAPKs-AP-1 signaling pathway (Reddy and Mossman, 2002; Tsai et al., 2007; Bergelson et al., 1994; Duvoix et al., 2004). However, the lack of change in JNK, ERK, and p38 phosphorylation in the presence of andrographolide in the present study (Fig. 1C), therefore, the possible involvement of MAPK signaling pathways in p-cJun was excluded and no MAPK inhibitors were tested. The results suggest that AP-1 activation is not likely to be via the MAPK pathway (Fig. 1C). Instead, we found that wortmannin and LY294002 suppressed the andrographolide-induced phosphorylation of Akt, which resulted in abolishing c-jun activation (Fig. 3) and AP-1 DNA-binding activity (Fig. 5A). Furthermore, the experiment with siPI3K clearly showed that knock down of PI3K expression abolishes the DNA-binding activity of AP-1 and also the induction of GSTP expression by andrographolide (Figs. 4D and 5B). Taken

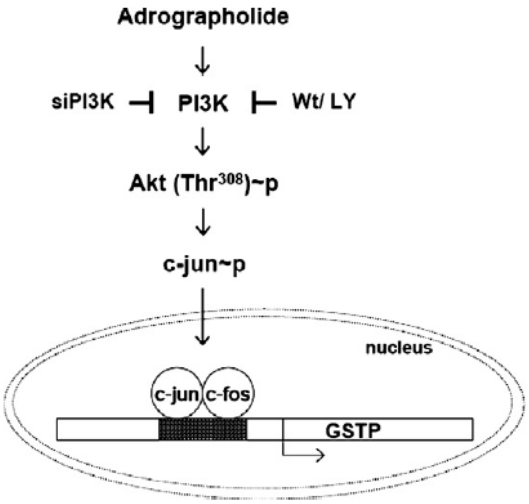

Fig. 8. Model showing the pathways that mediate andrographolide-induced GSTP expression in rat primary hepatocytes.

together, these data implicate the PI3K/Akt-AP-1 and not the MAPK-AP-1 signaling pathway in the andrographolide induction of GSTP gene expression.

The findings of the present study are summarized schematically in Fig. 8. We propose that andrographolide-induced GSTP expression is mediated by the PI3K/Akt signaling pathway and the AP-1 transcription factor in rat primary hepatocytes.

Conflict of Interest

The authors declare that they have no conflicts of interest associated with this work.

Acknowledgment

This work was supported by NSC-97-2320-B-039-047-MY3.

References

Abu-Ghefreh, A.A., Canatan, H., Ezeamuzie, C.I., 2009. In vitro and in vivo anti-inflammatory effects of andrographolide. International Immunopharmacology 9, 313–318.

Alessi, D.R., James, S.R., Downes, C.P., Holmes, A.B., Gaffney, P.R., Reese, C.B., Cohen, P., 1997. Characterization of a 3-phosphoinositide-dependent protein kinase which phosphorylates and activates protein kinase B alpha. Current Biology 7, 261–269.

Andjelkovic, M., Alessi, D.R., Meier, R., Fernandez, A., Lamb, N.J., Frech, M., Cron, P., Cohen, P., Lucocq, J.M., Hemmings, B.A., 1997. Role of translocation in the activation and function of protein kinase B. The Journal of Biological Chemistry 272, 31515–31524.

Angel, P., Imagawa, M., Chiu, R., Stein, B., Imbra, R.J., Rahmsdorf, H.J., Jonat, C., Herrlich, P., Karin, M., 1987. Phorbol ester-inducible genes contain a common cis element recognized by a TPA-modulated trans-acting factor. Cell 49, 729–739.

Angel, P., Karin, M., 1991. The role of Jun, Fos and the AP-1 complex in cell-proliferation and transformation. Biochimica et Biophysica Acta 1072, 129–157.

Bergelson, S., Pinkus, R., Daniel, V., 1994. Induction of AP-1 (Fos/Jun) by chemical agents mediates activation of glutathione S-transferase and quinone reductase gene expression. Oncogene 9, 565–571.

Borde-Chiche, P., Diederich, M., Morceau, F., Wellman, M., Dicato, M., 2001. Phorbol ester responsiveness of the glutathione S-transferase P1 gene promoter involves an inducible c-jun binding in human K562 leukemia cells. Leukemia Research 25, 241–247.

Chang, K.T., Lii, C.K., Tsai, C.W., Yang, A.J., Chen, H.W., 2008. Modulation of the expression of the pi class of glutathione S-transferase by *Andrographis paniculata* extracts and andrographolide. Food Chemical Toxicology 46, 1079–1088.

Chen, C., Kong, A.N., 2005. Dietary cancer-chemopreventive compounds: from signaling and gene expression to pharmacological effects. Trends in Pharmacological Sciences 26, 318–326.

Chen, H.W., Yang, J.J., Tsai, C.W., Wu, J.J., Sheen, L.Y., Ou, C.C., Lii, C.K., 2001. Dietary fat and garlic oil independently regulate hepatic cytochrome p(450) 2B1 and the placental form of glutathione S-transferase expression in rats. The Journal of Nutrition 131, 1438–1443.

Chen, J.H., Hsiao, G., Lee, A.R., Wu, C.C., Yen, M.H., 2004. Andrographolide suppresses endothelial cell apoptosis via activation of phosphatidyl inositol-3-kinase/Akt pathway. Biochemical Pharmacology 67, 1337–1345.

Chen, L.X., Qu, G.X., Qiu, F., 2006a. Studies on diterpenoids from *Andrographis paniculata*. Zhongguo Zhong Yao Za Zhi 31, 1594–1597. Chinese.

Chen, L.X., Qu, G.X., Qiu, F., 2006b. Studies on flavonoids of *Andrographis paniculata*. Zhongguo Zhong Yao Za Zhi 31, 391–395. Chinese.

Cheng, W.L., Lii, C.K., Chen, H.W., Lin, T.H., Liu, K.L., 2004. Contribution of conjugated linoleic acid to the suppression of inflammatory responses through the regulation of the NF-kappaB pathway. Journal of Agricultural and Food Chemistry 52, 71–78.

Choi, B.H., Kim, C.G., Lim, Y., Shin, S.Y., Lee, Y.H., 2008. Curcumin down-regulates the multidrug-resistance mdr1b gene by inhibiting the PI3K/Akt/NF kappa B pathway. Cancer Letters 259, 111–118.

De Bosscher, K., Vanden Berghe, W., Haegeman, G., 2003. The interplay between the glucocorticoid receptor and nuclear factor-kappaB or activator protein-1: molecular mechanisms for gene repression. Endocrine Reviews 24, 488–522.

Duvoix, A., Schnekenburger, M., Delhalle, S., Blasius, R., Borde-Chiche, P., Morceau, F., Dicato, M., Diederich, M., 2004. Expression of glutathione S-transferase P1–1 in leukemic cells is regulated by inducible AP-1 binding. Cancer Letters 216, 207–219.

Fang, J., Xia, C., Cao, Z., Zheng, J.Z., Reed, E., Jiang, B.H., 2005. Apigenin inhibits VEGF and HIF-1 expression via PI3K/AKT/p70S6K1 and HDM2/p53 pathways. FASEB Journal 19, 342–353.

Hayes, J.D., Pulford, D.J., 1995. The glutathione S-transferase supergene family: regulation of GST and the contribution of the isoenzymes to cancer chemoprotection and drug resistance. Critical Reviews in Biochemistry and Molecular Biology 30, 445–600.

Henderson, C.J., McLaren, A.W., Moffat, G.J., Bacon, E.J., Wolf, C.R., 1998. Pi-class glutathione S-transferase: regulation and function. Chemico-Biological Interactions 111–112, 69–82.

Hou, C.H., Hou, S.M., Tang, C.H., 2009. Ultrasound increased BMP-2 expression via PI3K, Akt, c-Fos/c-Jun, and AP-1 pathways in cultured osteoblasts. Journal of Cellular Biochemistry 106, 7–15.

Jarukamjorn, K., Don-in, K., Makejaruskul, C., Laha, T., Daodee, S., Pearaksa, P., Sripanidkulchai, B.O., 2006. Impact of *Andrographis paniculata* crude extract on mouse hepatic cytochrome P450 enzymes. Journal of Ethnopharmacology 105, 464–467.

Kapil, A., Koul, I.B., Banerjee, S.K., Gupta, B.D., 1993. Antihepatotoxic effects of major diterpenoid constituents of *Andrographis paniculata*. Biochemical Pharmacology 46, 182–185.

Laemmli, U.K., 1970. Cleavage of structural proteins during the assembly of the head of bacteriophage T4. Nature 227, 680–685.

Lee, Y.C., Lin, H.H., Hsu, C.H., Wang, C.J., Chiang, T.A., Chen, J.H., 2010. Inhibitory effects of andrographolide on migration and invasion in human non-small cell lung cancer A549 cells via down-regulation of PI3K/Akt signaling pathway. European Journal of Pharmacology 632, 23–32.

Li, J., Cheung, H.Y., Zhang, Z., Chan, G.K., Fong, W.F., 2007. Andrographolide induces cell cycle arrest at G2/M phase and cell death in HepG2 cells via alteration of reactive oxygen species. European Journal of Pharmacology 568, 31–44.

Li, J., Luo, L., Wang, X., Liao, B., Li, G., 2009. Inhibition of NF-kappaB expression and allergen-induced airway inflammation in a mouse allergic asthma model by andrographolide. Cellular and Molecular Immunology 6, 381–385.

Lii, C.K., Liu, K.L., Cheng, Y.P., Lin, A.H., Chen, H.W., Tsai, C.W., 2010. Sulforaphane and α-lipoic acid upregulate the expression of the π class of glutathione *S*-transferase through c-Jun and Nrf2 activation. The Journal of Nutrition 140, 885–892.

Liu, X.P., Goldring, C.E., Wang, H.Y., Copple, I.M., Kitteringham, N.R., Park, B.K., 2009. Extract of *Ginkgo biloba* induces glutathione-S-transferase subunit-P1 in vitro. Phytomedicine 16, 451–455.

Lu, S.C., 1999. Regulation of hepatic glutathione synthesis: current concepts and controversies. FASEB Journal 13, 1169–1183.

Manson, M.M., Foreman, B.E., Howells, L.M., Moiseeva, E.P., 2007. Determining the efficacy of dietary phytochemicals in cancer prevention. Biochemical Society Transactions 35, 1358–1363.

Martin, D., Rojo, A.I., Salinas, M., Diaz, R., Gallardo, G., Alam, J., De Galarreta, C.M., Cuadrado, A., 2004. Regulation of heme oxygenase-1 expression through the phosphatidylinositol 3-kinase/Akt pathway and the Nrf2 transcription factor in response to the antioxidant phytochemical carnosol. The Journal of Biological Chemistry 279, 8919–8929.

Milbury, P.E., Graf, B., Curran-Celentano, J.M., Blumberg, J.B., 2007. Bilberry (*Vaccinium myrtillus*) anthocyanins modulate heme oxygenase-1 and glutathione S-transferase-pi expression in ARPE-19 cells. Investigative Ophthalmology and Visual Science 48, 2343–2349.

Nadori, F., Lardeux, B., Rahmani, M., Bringuier, A., Durand-Schneider, A.M., Bernuau, D., 1997. Presence of distinct AP-1 dimers in normal and transformed rat hepatocytes under basal conditions and after epidermal growth factor stimulation. Hepatology 26, 1477–1483.

Neergheen, V.S., Bahorun, T., Taylor, E.W., Jen, L.S., Aruoma, O.I. 2009. Targeting specific cell signaling transduction pathways by dietary and medicinal phytochemicals in cancer chemoprevention. Toxicology doi:10.1016/j.tox.2009.10.010.

Okuda, A., Imagawa, M., Maeda, Y., Sakai, M., Muramatsu, M., 1989. Structural and functional analysis of an enhancer GPEI having a phorbol 12-O-tetradecanoate 13-acetate responsive element-like sequence found in the rat glutathione transferase P gene. The Journal of Biological Chemistry 264, 16919–16926.

Perez-Carreon, J.I., 2009. Tumor promoting and co-carcinogenic effects in medium-term rat hepatocarcinogenesis are not modified by co-administration of 12 pesticides in mixture at acceptable daily intake. Food Chemical Toxicology 47, 540–546.

Qin, L.H., Kong, L., Shi, G.J., Wang, Z.T., Ge, B.X., 2006. Andrographolide inhibits the production of TNF-alpha and interleukin-12 in lipopolysaccharide-stimulated macrophages: role of mitogen-activated protein kinases. Biological and Pharmaceutical Bulletin 29, 220–224.

Reddy, S.P., Mossman, B.T., 2002. Role and regulation of activator protein-1 in toxicant-induced responses of the lung. American Journal of Physiology 283, L1161–1178.

Rosseland, C.M., Wierod, L., Flinder, L.I., Oksvold, M.P., Skarpen, E., Huitfeldt, H.S., 2008. Distinct functions of H-Ras and K-Ras in proliferation and survival of primary hepatocytes due to selective activation of ERK and PI3K. Journal of Cellular Physiology 215, 818–826.

Roy, P., Kalra, N., Prasad, S., George, J., Shukla, Y., 2009. Chemopreventive potential of resveratrol in mouse skin tumors through regulation of mitochondrial and PI3K/AKT signaling pathways. Pharmaceutical Research 26, 211–217.

Sakai, M., Okuda, A., Muramatsu, M., 1988. Multiple regulatory elements and phorbol 12-O-tetradecanoate 13-acetate responsiveness of the rat placental glutathione transferase gene. Proceedings of the National Academy of Sciences of the United States of America 85, 9456–9460.

Seglen, P.O., 1976. Preparation of isolated rat liver cells. Methods in Cell Biology 13, 29–83.

Sheehan, D., Meade, G., Foley, V.M., Dowd, C.A., 2001. Structure, function and evolution of glutathione transferases: implications for classification of non-mammalian members of an ancient enzyme superfamily. The Biochemical Journal 360, 1–16.

Shen, Y.C., Chen, C.F., Chiou, W.F., 2000. Suppression of rat neutrophil reactive oxygen species production and adhesion by the diterpenoid lactone andrographolide. Planta Medica 66, 314–317.

Singh, R.P., Banerjee, S., Rao, A.R., 2001. Modulatory influence of *Andrographis paniculata* on mouse hepatic and extrahepatic carcinogen metabolizing enzymes and antioxidant status. Phytotherapy Research 15, 382–390.

Stephens, L., Anderson, K., Stokoe, D., Erdjument-Bromage, H., Painter, G.F., Holmes, A.B., Gaffney, P.R., Reese, C.B., McCormick, F., Tempst, P., Coadwell, J., Hawkins, P.T., 1998. Protein kinase B kinases that mediate phosphatidylinositol 3,4,5-trisphosphate-dependent activation of protein kinase B. Science 279, 710–714.

Surh, Y.J., 2003. Cancer chemoprevention with dietary phytochemicals. Nature Reviews 3, 768–780.

Tsai, C.W., Chen, H.W., Yang, J.J., Liu, K.L., Lii, C.K., 2005. Sulfur amino acid restriction induces the pi class of glutathione S-transferase expression in primary rat hepatocytes. The Journal of Nutrition 135, 1034–1039.

Tsai, C.W., Chen, H.W., Yang, J.J., Sheen, L.Y., Lii, C.K., 2007. Diallyl disulfide and diallyl trisulfide up-regulate the expression of the pi class of glutathione S-transferase via an AP-1-dependent pathway. Journal of Agricultural and Food Chemistry 55, 1019–1026.

van Iersel, M.L., Verhagen, H., van Bladeren, P.J., 1999. The role of biotransformation in dietary (anti)carcinogenesis. Mutation research 443, 259–270.

Visen, P.K., Shukla, B., Patnaik, G.K., Dhawan, B.N., 1993. Andrographolide protects rat hepatocytes against paracetamol-induced damage. Journal of Ethnopharmacology 40, 131–136.

Wierod, L., Rosseland, C.M., Lindeman, B., Oksvold, M.P., Grosvik, H., Skarpen, E., Huitfeldt, H.S., 2007. CDK2 regulation through PI3K and CDK4 is necessary for cell cycle progression of primary rat hepatocytes. Cell Proliferation 40, 475–487.

Woo, A.Y., Waye, M.M., Tsui, S.K., Yeung, S.T., Cheng, C.H., 2008. Andrographolide up-regulates cellular-reduced glutathione level and protects cardiomyocytes against hypoxia/reoxygenation injury. The Journal of Pharmacology and Experimental Therapeutics 325, 226–235.

World Health Organization, 2002. WHO Monographs on Selected Medicinal Plants, vol 2. World Health Organization, Geneva, Switzerland. pp. 12–24.

Xia, Y.F., Ye, B.Q., Li, Y.D., Wang, J.G., He, X.J., Lin, X., Yao, X., Ma, D., Slungaard, A., Hebbel, R.P., Key, N.S., Geng, J.G., 2004. Andrographolide attenuates inflammation by inhibition of NF-kappa B activation through covalent modification of reduced cysteine 62 of p50. Journal of Immunology 173, 4207–4217.

Xu, C., Li, C.Y., Kong, A.N., 2005. Induction of phase I, II and III drug metabolism/transport by xenobiotics. Archives of Pharmacal Research 28, 249–268.

Yang, A.J., Li, C.C., Lu, C.Y., Liu, K.L., Tsai, C.W., Lii, C.K., Chen, H.W., 2010. Activation of the cAMP/CREB/inducible cAMP early repressor pathway suppresses andrographolide-induced gene expression of the pi class of glutathione S-transferase in rat primary hepatocytes. Journal of Agricultural and Food Chemistry 58, 1993–2000.

Yu, A.L., Lu, C.Y., Wang, T.S., Tsai, C.W., Liu, K.L., Cheng, Y.P., Chang, H.C., Lii, C.K., Chen, H.W., 2010. Induction of heme oxygenase 1 and inhibition of tumor necrosis factor alpha-induced intercellular adhesion molecule expression by andrographolide in EA.hy926 cells. Journal of Agricultural and Food Chemistry 58, 7641–7648.

Zablotowicz, R.M., Hoagland, R.E., Locke, M.A., Hickey, W.J., 1995. Glutathione-S-transferase activity and metabolism of glutathione conjugates by rhizosphere bacteria. Applied and Environmental Microbiology 61, 1054–1060.

Zhou, J., Ong, C.N., Hur, G.M., Shen, H.M., 2010. Inhibition of the JAK-STAT3 pathway by andrographolide enhances chemosensitivity of cancer cells to doxorubicin. Biochemical Pharmacology 79, 1242–1250.

國科會補助專題研究計畫成果報告自評表

請就研究內容與原計畫相符程度、達成預期目標情況、研究成果之學術或應用價值（簡要敘述成果所代表之意義、價值、影響或進一步發展之可能性）、是否適合在學術期刊發表或申請專利、主要發現或其他有關價值等，作一綜合評估。

1. 請就研究內容與原計畫相符程度、達成預期目標情況作一綜合評估

■達成目標

□ 未達成目標（請說明，以 100 字為限）

□ 實驗失敗

□ 因故實驗中斷

□ 其他原因

說明：

2. 研究成果在學術期刊發表或申請專利等情形：

論文：■已發表 □未發表之文稿 □撰寫中 □無

專利：□已獲得 □申請中 □無

技轉：□已技轉 □洽談中 □無

其他：（以 100 字為限）

3. 請依學術成就、技術創新、社會影響等方面，評估研究成果之學術或應用價值（簡要敘述成果所代表之意義、價值、影響或進一步發展之可能性）（以 500 字為限）

穿心蓮在中國、韓國和印度等亞洲國家已是廣泛被應用的傳統中草藥，具有抗肝毒性、抗病毒與抗發炎等效果。穿心蓮內酯是目前被發現穿心蓮中最具有生理活性的成分之一，屬於 bicycle diterpenoid lactone，主要分布在穿心蓮葉子中。根據本研究的成果發現，穿心蓮內酯具有促進肝臟解毒酵素表現的功能。在現今健康意識抬頭，大眾對保健食品的接受度及需求量增加，若將穿心蓮發展成保健食品，一能將中國傳統中草藥推向國際被廣泛接受，二能透過天然草藥中的有效成分增加肝臟解毒代謝的能力，降低肝臟受到外來異物的傷害，會比服用合成藥物讓人感到更加安心。